NASA TM X-56024

INITIAL RESULTS FROM FLIGHT TESTING A LARGE, REMOTELY PILOTED AIRPLANE MODEL

Compiled by Euclid C. Holleman

March 1974

NASA high-number Technical Memorandums are issued to provide rapid transmittal of technical information from the researcher to the user. As such, they are not subject to the usual NASA review process.

NASA Flight Research Center
Edwards, California 93523

INITIAL RESULTS FROM FLIGHT TESTING A LARGE, REMOTELY PILOTED AIRPLANE MODEL

Compiled by Euclid C. Holleman
Flight Research Center

ABSTRACT

The first four flights of a remotely piloted airplane model showed that a flight envelope can be expanded rapidly and that hazardous flight tests can be conducted safely with good results. The flights also showed that aerodynamic data can be obtained quickly and effectively over a wide range of flight conditions, clear and useful impressions of handling and controllability of configurations can be obtained, and present computer and electronic technology provide the capability to close flight control loops on the ground, thus providing a new method of design and flight test for advanced aircraft.

INTRODUCTION

Most airplanes are subject to uncontrollable stall and/or departure, perhaps even spin, when maneuvered to critically high angles of attack. Some airplanes, notably transports, can be designed to perform their missions without entering the high-angle-of-attack problem area. Other airplane missions, those of fighter airplanes, for example, require that the airplane operate over the entire flight envelope capability of the design. Thus control problems at high angle of attack, if they exist, are encountered on an operational basis. Loss of control at high angle of attack in these types of airplanes can result in intolerable loss in effectiveness and perhaps loss of the airplane. These losses have emphasized the need to design for normal flight controllability at high angle of attack.

High-performance airplane design and operational checkout usually include an investigation of stall, departure, spin, and recovery with scaled models and later with the actual airplane. Flight regions where intolerable control problems are likely are determined and, if required, modifications are proposed to make the airplane acceptable for its design mission. In many instances the correlation between scaled-model behavior at high angle of attack and the airplane behavior

has been satisfactory, but in other instances correlation has been less than satisfactory, for example, designs which have high fuselage loading compared to loading distributed along the wing (ref. 1). Therefore a need exists for a better understanding of design for high-angle-of-attack controllability and for investigations into the reasons for less than satisfactory correlation of scaled-model to full-scale flight.

The NASA Flight Research Center is flight testing a large-scale model of the F-15 airplane in an effort to correlate model and full-scale flight stall, departure, and spin controllability considering the effects of dynamic scaling laws and Reynolds number. The three-eighth-scale model was constructed to be geometrically similar to the full-scale airplane, and the inertial and mass characteristics were scaled to within known correctable tolerance of the full-scale airplane. Tests are planned with a second model with more closely scaled mass and inertia characteristics. The remotely piloted method of flight test was selected for the program, reasoning that if high risk departure and spin tests could be accomplished with less expensive models and test methods, it would be desirable to do so. In addition, the remotely piloted method allows the versatility of testing with a pilot in control as would be done during normal flight test and also allows the effect of advanced control systems to be determined. Feedback loops designed for the normal flight envelope sometimes command surface motions that augment rather than oppose spin motions. The large model was selected to provide (1) data nearer full-scale flight Reynolds numbers for correlation and (2) model handling within the normal control capability of the pilot with the scale factors required for dynamic modeling (ref. 2).

The first flight was made on October 12, 1973, and the fourth flight was made on December 21, 1973. These flights essentially covered the model flight envelope and were made to check out operational procedures and verify the aerodynamic similarity of the three-eighth-scale-model data to small-scale wind-tunnel data. This report briefly describes the scaled model, instrumentation, control system mechanization, and operational procedures, and presents typical flight data and pilot evaluations of the effectiveness of the test method.

Sections of this paper were contributed by John W. Edwards, Kenneth W. Iliff and Richard E. Maine, Einar K. Enevoldson, Garrison P. Layton, and Jon L. Ball.

SYMBOLS

Values are given in the International System of Units (SI) and parenthetically in U.S. Customary Units. Measurements and calculations were made in U.S. Customary Units.

a_n normal acceleration at the center of gravity, g

a_y lateral acceleration at the center of gravity, g

C_L lift coefficient, $\frac{\text{Lift}}{\bar{q}S}$

C_{l_β}	roll due to sideslip derivative, per deg
C_{l_p}	roll damping derivative, per radian
C_m	pitching moment coefficient, $\frac{\text{Pitching moment}}{\bar{q}Sc}$
C_{m_q}	pitch damping derivative, per radian
C_{m_α}	static longitudinal stability derivative, per deg
C_{n_β}	static directional stability derivative, per deg
c	wing reference chord, m (ft)
g	acceleration due to gravity, 9.8 m/sec^2 (32.2 ft/sec^2)
I_X	moment of inertia about the longitudinal body axis, kg-m^2 (slug-ft^2)
I_{XZ}	product of inertia, kg-m^2 (slug-ft^2)
I_Y	moment of inertia about the lateral body axis, kg-m^2 (slug-ft^2)
I_Z	moment of inertia about the normal body axis, kg-m^2 (slug-ft^2)
p	rolling velocity, deg/sec
q	pitching velocity, deg/sec
$\bar{q}$	dynamic pressure, N/m^2 (lb/ft^2)
r	yawing velocity, deg/sec
S	wing reference area, m^2 (ft^2)
t	time, sec
V	velocity, m/sec (ft/sec)
α	angle of attack, deg
β	angle of sideslip, deg

δ_a	aileron position, deg
$(\delta_a)_c$	roll control command signal
δ_{a_p}	pilot's lateral stick position, cm (in.)
δ_d	rolling tail differential position, deg
δ_h	average of two horizontal stabilizer positions, deg
$(\delta_{h_L})_c$	left horizontal stabilizer command signal
$(\delta_{h_R})_c$	right horizontal stabilizer command signal
δ_r	rudder position, deg
$(\delta_r)_c$	yaw control command signal
θ	pitch attitude angle, deg
φ	roll attitude angle, deg
ψ	heading angle, deg

REMOTELY PILOTED FLIGHT SYSTEM

Base Model

The F-15 airplane was designed as a conventional single-place advanced air superiority fighter airplane with a 45° leading-edge-sweep wing, two engines, and twin vertical tails. The model (figs. 1 and 2) was molded to the scaled contours of the full-scale airplane and was built primarily of fiber glass with metal load-carrying members in each section. It was built to be as stiff as the airplane and to be capable of withstanding normal loads five times normal 1g flight. No propulsion was provided. Inlets were drooped 11° to simulate the low-speed, high-angle-of-attack flight configuration. Otherwise, the model simulated the airplane clean configuration without landing gear and flaps. The inlet ducts were blocked approximately 2.97 meters (117 inches) aft of the nose, just inside the inlet lip, by a flat plate normal to the duct. The tailpipes housed drogue and recovery parachutes. The aileron, rudder, and horizontal tail control surfaces were actuated by nonredundant hydraulic actuators providing aerodynamic control. Control deflection limits were the same as for the full-scale airplane (table 1). Batteries powered all

on-board systems including the hydraulic system. Dimensions, weight, and inertia of the model are summarized in table 1.

A parachute system was used to recover the model. The system was activated by a dualized pyrotechnic system and was composed of a 3.66-meter- (12-foot-) diameter drogue parachute for initial deceleration of the model, a 24.27-meter- (79.6-foot-) diameter main parachute for final descent, and a 5.49-meter- (18-foot-) diameter engagement parachute for the mid-air retrieval system (MARS). A 1.83-meter- (6-foot-) diameter stabilization parachute steadied the model while it was being towed under the recovery helicopter. The parachute recovery sequence was initiated by one of the following: radio frequency loss, remote pilot command, dynamic pressure over a preset design value, and altitude less than 4570 meters (15,000 feet).

A wings-leveling autopilot function was activated by temporary radio frequency loss to prevent nuisance deployment of the recovery system. All on-board avionics (including downlink and autopilot) except the parachute pyrotechnic system were nonredundant. Complete reliance was placed in the parachute recovery system to retrieve the model in the event of system failures. The design philosophy required that the model only receive control commands and actuate the controls. All inter-flight changes required of the avionics and control systems were to be accomplished in the ground computer, a more flexible and easily modified function.

Instrumentation

A block diagram of the model instrumentation system is shown in figure 3. Twenty-two model response and control quantities, angular rates and attitude, linear accelerations, velocity, altitude, and control surface positions were sensed as well as 25 operational quantities. The data were transmitted to the ground via pulse code modulation (PCM) telemetry for display and recording. Actual parameters, ranges of the parameters, and analog prefilter frequencies are listed in table 2. The resolution of the recorded quantities is also given. Each quantity was transmitted at a sample rate of 200 per second. In addition to the flight quantities, the pilot's cockpit control positions and cockpit switch positions were recorded. The flights were also tracked by radar.

Postflight digital data processing routines applied a digital filter with a notch at 19 hertz and a third-order low-pass filter at 20 hertz to reduce the structural noise that was picked up by the data sensors primarily above 15° angle of attack. Additional digital data processing routines applied calibrations to the raw data, corrected angle of attack and angle of sideslip for local flow deflection, angular rates, and linear accelerations, and converted total and static pressure to the conventional air data functions.

In addition to the analog prefiltering for the PCM system on board the model, notch and low-pass filters were used in the real-time digital data processing program to reduce the structural noise near 20 hertz in the acceleration and rate data.

Remote Control Loops

A block diagram of the remotely piloted system (ref. 3) is shown in figure 4. The model response variables are telemetered to the ground station where they are routed to the ground computer, the ground cockpit instrument panel, and analog strip chart recorders for real-time flight monitoring. At the ground station, the ground cockpit proportional control functions (stick and pedals) are processed by the analog-to-digital converter and are trunked to the ground computer together with the mode panel signals. The ground computer calculates the command variables and provides them to the uplink encoder. The remotely piloted flight system uses two uplink encoders. The computer encoder receives command variables from the computer, and the bypass encoder receives command variables directly from the ground cockpit. The pilot selects an encoder by means of a pushbutton on the mode control panel. The bypass encoder serves as a backup to the computer encoder if the computer malfunctions. The command signals are transmitted to the model where they are decoded and sent to the appropriate servo channel.

Closing the piloting control loop on the ground has an obvious advantage. Only relatively simple flight systems are required in the air vehicle with readily available simulation type hardware on the ground to complete the control loops.

The telemetry link operation is sensitive to such factors as the attitude of the model and atmospheric conditions. The telemetry links are essentially "line-of-sight" transmission paths, and the signal may be blocked by the model wing or by flying behind a hill or below the horizon at extreme range. It was anticipated that flight operations would be limited to approximately 55.5 kilometers (30 miles) from the ground station with the model flying at altitudes between 1500 meters (5000 feet) and 2100 meters (7000 feet). The range can be extended to approximately 185 kilometers (100 miles) if the model flies at an altitude of approximately 12,200 meters (40,000 feet).

Telemetry downlink.– The existing Flight Research Center's telemetry flight data acquisition system was used for the telemetry downlink. This system provided aircraft response variables to the ground station at 200 samples per second. The characteristics of this pulse-code-modulation system are listed in table 3. The model was fully instrumented with a 40-hertz first-order-lag analog prefilter on all channels. The low-power level (5 watts) and the lack of parity check on the downlink indicated the need for reasonability checks in the software to discriminate against bad telemetry data.

Telemetry uplink.– The telemetry uplink used for the system was developed by the U.S. Navy for the remote control of drone aircraft. The system is capable of several modes of operation, from the control of a single drone to the time-multiplexed control of a fleet of drones. Because it can control more than one drone simultaneously, the update rate of the system when controlling a single aircraft is comfortably high. Consequently, the system has good research capability.

The uplink telemetry cycle (fig. 5) consists of four 16-bit proportional data words (frames) and a sync word transmitted at 53.33 samples per second (18.75 milliseconds cycle time). Each 16-bit word is coded as two 9-bit bytes containing a

parity bit, with each frame requiring 3.75 milliseconds. The four data words are aileron command, $(\delta_a)_c$, left stabilizer command, $(\delta_{h_L})_c$, right stabilizer command, $(\delta_{h_R})_c$, and rudder command, $(\delta_r)_c$. The uplink command words are the 10 most significant bits of the 16-bit data words. The remaining 6 bits of each frame are available to be used as discrete signals to the model. The sync word contains a specific bit structure which the receiver-decoder in the model tests to determine that the system is synchronized.

The telemetry uplink system operates from a 50-watt transmitter which transmits through a directional parabolic antenna with a 12-decibel gain. The antenna is slaved to a radar antenna which tracks the model. The transmission is on a UHF band frequency and utilizes frequency shift key coding.

Intermittent dropout of the telemetry uplink signal was not expected to cause serious problems because of the parity checking in the decoder; however, loss of the telemetry uplink carrier signal for 0.5 second would cause the model to switch to the on-board autopilot mode.

Computer.– The computer used in the system is a general-purpose minicomputer with a 16K memory consisting of 16-bit words. The computer has a 750 nanosecond cycle time. The peripheral equipment, software, and main-frame options of the computer are listed in table 4.

As an indication of the capability of the computer to perform feedback control law computations, the time required for the computer to sum two feedback variables and a pilot command signal (each multiplied by a gain) and to operate on the resulting error signal with a first-order digital filter is approximately 0.7 millisecond.

The telemetry uplink sample rate for 53.33 samples per second sets the sample rate of the overall digital control system. The telemetry downlink data are input to the ground computer at its rate of 200 samples per second, but only one sample of every four is used in the control law computation. The control law computation performed by the FORTRAN main program is driven by the uplink encoder interrupt which requests one of the control surface commands every 3.75 milliseconds (fig. 5). Thus the control system is functionally equivalent to an on-board digital fly-by-wire system operating at a sample rate of 53.33 samples per second.

Control Systems

A unique feature of the remote pilot concept of this program was the use of a ground computer to digitally mechanize the control system for the model. The research nature of the program required several different control system modes which were selected by the pilot through the mode control panel (fig. 6). Four modes were implemented in each of the pitch, roll, and yaw axes: computer direct, rate damper, mechanical control system, and control augmentation system. The latter two modes are the full-scale airplane's control system. When the model

is flown in these modes, the ground based computer simulates the gearing schedules, actuator and filter dynamics, and augmentation of the full-scale airplane. The mechanical control system mode is the "open loop" unaugmented mode, whereas the control augmentation system mode adds angular rate and acceleration augmentation to the mechanical control system commands.

The computer direct and rate damper modes were implemented to provide a simple control system without the need to simulate a full-scale airplane control system mode. The computer direct mode provided open-loop proportional control, and the rate damper mode added simple rate dampers onto the computer direct mode gearing.

The FORTRAN control program of the ground computer was checked out and debugged using the Flight Research Center's real-time digital simulation facility. Subroutines were written for the simulation computer to simulate the computer ASSEMBLY subroutines which provide the input/output of data to the FORTRAN card deck to be used for both the computer and the simulation. This capability is a great aid in debugging and modifying the program. Thus far in the flight program, a number of modifications have been made to the program between flights. As an example, between flights 2 and 3, seven digital filters were added to the program to implement the rate damper mode.

Another unique feature of the computer-mechanized control system was the step input switches to command step control surface deflections for recording model response data. The control panel for these switches was on the pilot's left console and provided a convenient and practical way of making control inputs.

Actual model control system hardware limits, rate limits, and response characteristics as well as the scaled feedback loop characteristics were mechanized on the digital computer. All actual airplane control surface deflection limits were adhered to.

Ground Facility Implementation

A thorough, straightforward engineering design was used to implement the ground facility. The first flights were flown successfully from the facility; however, time and experience dictated modifications to improve the operation. Timing and noise problems have been encountered that were of a higher magnitude than initially expected and were manifested in the most subtle manner.

As can be seen in figure 4, the ground facility was a fairly complex integration of analog and digital equipment. Wherever possible, major existing units were used, which necessitated special interface/buffer equipment. Hardware transmission distances varied from a few meters to 750 meters (2500 feet). Transmission techniques varied from wide band video amplifiers for television and digital differential line drivers and receivers for digital information to specialized balanced and compensated line amplifiers for uplink modulation. A passive antenna relay system was successfully implemented to facilitate radio frequency ground checkout while the model was in a shielded hangar.

Equipment with logic speeds varying from 150 K Hz to 10 M Hz was integrated by trial methods. Operational configurations did not necessarily conform to original designs nor lend themselves to clear-cut analysis. Digital pulse widths were optimized, with changes predicated on the equipment. Clock frequencies were varied to decrease the number of simultaneous interrupts to the computer, and sequence-locked switching of the uplink encoders was instituted to insure that command information was not transposed when going from computer modes to bypass mode.

Another anticipated modification will be to install peripheral buffer registers between equipment and computer input lines to relieve part of the timing problem and release needed time in the control law computer central processor.

Control Station

The control station was composed of the pilot's ground cockpit (fig. 7), the flight engineer's station, and two observer posts, all housed in a closed, insulated room within the ground facility. Two communication links were used in the control station. The pilot used UHF radio to talk to the flight controller, to the launch, chase, and recovery aircraft, and to air traffic control agencies. The flight engineer used an intercom to talk to the flight director, range facilities director, and ground facility director, as well as to listen to UHF conversations.

The pilot's ground cockpit was configured much like a conventional fixed base simulator cockpit, although no particular aircraft cockpit was simulated. The displays included airspeed, altitude, rate of climb, angle of attack, angle of sideslip, yaw rate, pitch rate, normal acceleration, control positions, and commanded control position. These quantities were presented in conventional round-dial aircraft instrument face format. Aircraft attitude and heading were presented on a three-axis attitude indicator. All these instruments displayed processed telemetered data from the model.

A 23-centimeter (9-inch), 525-line, black-and-white television was displayed above the instrument panel. It showed the view from a forward-looking television camera located in the model cockpit. The television was used as a backup navigation and control display, and was to be the primary visual display if recovery parachute failure made an emergency landing necessary.

The pilot's primary controls were a conventional fighter airplane control stick and rudder pedals. Control feel was provided in each axis by a high-quality, computer-controlled, electric force-feel system. This system was capable of extensive adjustment, including control circuit inertias, viscous damping, breakout, dead band, gradients, and gearing. The feel system did not simulate the F-15 airplane but was adjusted to suit the model flight characteristics and the maneuvers planned for an individual flight. Pitch and roll were trimmed with a standard "coolie-hat" switch on the pilot's control stick. Yaw was trimmed with a toggle switch on the left instrument subpanel.

Control system modes were selected on a "keyboard" console by either the flight engineer or the pilot. Discrete commands, such as drogue parachute deploy, autopilot select, hydraulics off, electrical power off, and uplink antenna selector, were made with a set of guarded toggle switches on the instrument panel that were operated by either the pilot or the flight engineer. A set of status lights on the instrument panel indicated the state of the autopilot, recovery sequence, hydraulic system, electrical system, etc.

OPERATIONAL PROCEDURES

Preflight Preparation

All manned air-launched vehicle flights at the Flight Research Center are planned in detail on a fixed base flight procedural simulator to obtain as much flight data as possible during each flight. The pilot practices the flight plan before each flight to become thoroughly familiar with the flight. This procedure was also used in preparing for the model flights. The simulator was updated on an interflight basis to reflect control system changes and the best estimate of model aerodynamics based on data from previous flights. Fifteen to 20 hours of practice on the flight simulator thoroughly familiarized the pilot with the flight plan and allowed him to compress a high work load flight plan of about 40 individual maneuvers into a 7-minute flight. Even with this preparation for normal flights, in previous programs the pilots were usually more hurried during actual flight than during simulated flight. Similarly, the remote pilot of the model was also more hurried during actual flight than during simulated flight. Therefore, an increased simulation time scale was used to provide practice for the pilot at a more rapid pace than during actual flight. After considering several time factors faster than real time, a factor of 1.4 was accepted as providing satisfactory training.

Flight

The F-15 model was launched from a B-52 carrier airplane at an altitude of 13,700 meters (45,000 feet) and a Mach number of 0.65 with the horizontal stabilizer set at -0.6° and all other control surfaces locked at 0°. At launch the hydraulic valve was deenergized to lock the control actuators. Three seconds after launch the valve was energized and the pilot assumed control. The desired control mode was selected, and research maneuvers were performed much like flying a fixed base simulator. After the flight plan was completed, the recovery parachute sequence was initiated. Final recovery was made by MARS helicopter.

INITIAL RESULTS

The flight envelope of the third flight of the remotely piloted model is shown in figure 8. After launch the model was flown through the mechanical control system mechanization in the computer and data were recorded to be analyzed for

stability and control derivatives. The model was then trimmed to high angle of attack (approximately 28°) with the stability augmentation system on to record pulses for analysis. The model was lightly damped at high angle of attack, and the dampers were used in each axis that was not being disturbed for recording data maneuvers. With the mechanical control system and later with computer-direct controls, the pilot trimmed full back stick (-23° for the mechanical control system and -25° for computer direct) and evaluated the controllability at angles of attack from 28° to 30°. Full roll and yaw controls were used to assess model stability.

To determine the acceptability of the model in predicting F-15 airplane controllability, data from standard stability and control evaluation maneuvers were recorded. From these maneuvers the stability and control characteristics as well as the lift variation with angle of attack (fig. 9) of the model were determined for comparison with wind-tunnel-predicted characteristics of the airplane. All data presented are for low speeds representative of Mach 0.2 and are for near-trimmed flight. Cursory comparisons with some small-scale wind-tunnel results indicate acceptable agreement between the wind-tunnel data and the flight data. Note that zero lift occurs at a negative angle of attack and maximum lift is at about $C_L = 1.2$. The longitudinal control required to trim at a given angle of attack (fig. 10) shows two levels of apparent longitudinal stability. Whereas about 2° of angle-of-attack change result from 1° of elevator deflection at low angle of attack, the slope at high angle of attack is more nearly 1, thus indicating increased stability at high angle of attack or decreased control effectiveness. These indications also confirm some small-scale wind-tunnel results for the airplane. As expected, the calculation of $C_m(\alpha)$ (fig. 11) from these data also shows an increase in the level of longitudinal stability at the higher angles of attack.

Stability and Control Derivative Analysis

One of the more persistent challenges to flight test aerodynamicists has been the determination of the 20 or so stability and control derivatives that, in conjunction with the flight condition, enable the time response characteristics of the airplane in the linear range to be calculated. Methods, usually referred to as maximum likelihood estimators, have been derived recently that produce results with confidence and without grueling effort and subjective judgments on the part of the analyst. This method of analysis minimizes the difference between the flight time history and a calculated time history resulting from the set of determined derivatives. The maximum likelihood estimator used is described in detail in reference 4. In addition to the derivative estimates obtained by this method, confidence levels (analogous to the Cràmer-Rao bounds described in ref. 4) are also obtained. The confidence levels indicate the relative amount of information contained in each maneuver analyzed for each derivative.

A typical lateral and a typical longitudinal maneuver are shown in figures 12(a) and 12(b). The solid line represents the measured flight data, and the dotted line the computed data based on the estimated derivatives. The match of the two sets of data is excellent, which is one criterion for the successful extraction of stability derivative estimates. Another criterion is the confidence levels. Figure 13 shows

the estimated flight values of the derivatives C_{m_α}, C_{m_q}, C_{l_β}, C_{n_β}, and C_{l_p} as well as the associated confidence level for each maneuver analyzed. The confidence level is shown by the vertical line through each data point. The longer the line, the lower the confidence in a given derivative. Ideally the fairing for the derivative variation with angle of attack (solid line) would pass within the range of all the confidence levels indicated. The dashed line represents the wind-tunnel estimates for each derivative. Some differences between the two sets of estimates are evident for all the derivatives shown. Of particular significance is the difference in the two estimates of C_{l_β} and C_{n_β} at high angle of attack. The flight data predict greater lateral-directional static stability than the wind-tunnel data. This results in a better flying vehicle than originally predicted.

Only five representative derivative variations are presented, although a complete set was obtained from the analysis. The complete set of derivatives was used to update the flight support simulator between flights, providing the current best estimate of model handling for flight planning.

A significant advantage of the remotely piloted concept is that the flight envelope can be investigated in a single flight, inasmuch as pilot safety is of no concern. On the first flight, data for stability and control derivatives were obtained over an impressive angle-of-attack range of 4° to 22°. (Zero lift was at $\alpha = -2°$.) During the first four flights, 63 stability and control maneuvers were performed and 51 were successfully analyzed. These maneuvers covered an angle of attack range of 3° to 31°.

Damper System Operation

A unique feature of the remotely piloted model method of control was the capability of programing control systems on the ground based computer, which allowed the pilot to fly the augmented model as if the augmentation loops were closed within the airplane rather than through the remote command loops. Although experience has been obtained with the sophisticated controls designed for the F-15 airplane, examples of the operation of simple rate dampers in each of the three axes are shown to illustrate the capability and flexibility of the remotely piloted controls. The damping loops required filters to suppress a structural vibration at a frequency of about 20 hertz that was sensed by the rate gyros. The yaw axis was mechanized with a washout circuit to allow normal turns without damper action. Three low-pass filters, three notch filters, and one washout filter were used in the rate damper control system. These filters were all implemented as digital filters in the ground-based computer.

Example time histories of model time response to aerodynamic control surface doublets are shown in figure 14. Figure 14(a) shows the longitudinal response of the model to a stabilizer doublet and the operation of the pitch rate damper after several oscillations. The damper gain was 0.4 deg/deg/sec. Damping with the pitch damper operating was estimated to be about three times the basic model damping.

Lateral-directional maneuvers are shown in figure 14(b). Three responses to aileron, rudder, and rolling tail doublets exciting the unaugmented model are shown, with the model response being damped by the roll and yaw rate dampers between each maneuver. At the indicated angle of attack, the yaw rate damper is not effective in damping the coupled roll-yaw oscillation, but the roll damper is very effective. The roll and yaw damper gains were 0.8 and 1.0 deg/deg/sec, respectively, whereas the yaw rate washout had a 1.86-second time constant. Although the possibility of having bad downlink telemetry data for the computation of the closed-loop command signals was anticipated, no downlink telemetry data dropouts have occurred during closed-loop operation.

Control at High Angle of Attack

A prime objective of the program was to determine the controllability of the model at high angle of attack; consequently, the model longitudinal control was moved to full trailing edge up at slow and fast rates to determine the maximum angle of attack that could be reached. Figure 15 illustrates three of these maneuvers to high angle of attack. The first was made with the mechanical control system and shows a pullup rate of about 4 deg/sec with the maximum stabilizer available (-23°) being used. The maximum angle of attack was 31.3°. The basic airplane motion was very lightly damped (damping ratio calculated to be 0.02). At an angle of attack of 25° the pilot commanded full right aileron (10°). The mechanical control system had an aileron-to-rudder interconnect which commanded nearly full coordinating rudder (-28.7°) at the high-angle-of-attack, full-up stabilizer condition. The airplane responded by rolling and pitching. Bank angle and pitch angle reached approximately 90° and -90° within about 7 and 9 seconds, respectively. The model continued to roll to near wings level and was recovered to level flight at approximately the same heading as that at which the maneuver was entered. The model responded to both longitudinal and lateral control throughout the maneuver.

At $t \approx 25$ seconds the controls were switched to computer direct which allowed the pilot to command an additional -2° of stabilizer. A rapid pullup to full-trailing-edge-up stabilizer was made, with the rate of change of angle of attack reaching about 20 deg/sec. An angle-of-attack overshoot of approximately 8° above the 30° average angle of attack was reached. Only small control inputs were made as the model was allowed to stabilize at this condition. There were no divergences, and response to recovery control was rapid.

A pullup at a rate of change of angle of attack of about 10 deg/sec was made during the third maneuver of figure 15 ($t = 60$ sec). The average angle of attack was 30°. The model was allowed to stabilize, and responses to pulses were recorded for analysis. Toward the end of the maneuvers, the pilot made a maximum aileron deflection right roll. The model responded to a bank angle of about 80°, and a pitch down to recover was made. A right yaw rate of 20 deg/sec was recorded, but there was no out-of-control departure. The drogue parachute opened at $t = 90$ seconds, ending the flight. A large part of the angle-of-attack envelope capability of the model was explored in the last 2 minutes of the flight.

Impressions of Remote Piloting

Prior to this program, limited experience with remotely piloted flight indicated that the versatility of the pilot provided a capability that could be used to advantage. With proper stimuli and motivation, the remote pilot could "fly" a desired flight plan and, if required, alter the plan to save a flight that might be lost. Since the approach is like simulation, the display stimuli may be as realistic as practical considerations permit. Experience has shown that piloting cues from a fixed base simulator are satisfactory for most flight situations except, perhaps, the flare to land.

After four flights, many impressions of the remotely piloted test method have been formed. Some impressions are summarized here. More complete pilot comments are given in the appendix as they were recorded.

The flights have been efficient in producing much good quality data in a short time. Extensive simulation has resulted in a well-practiced and well-rehearsed crew for each flight. The flexibility of the control system has permitted a useful degree of tailoring on each flight. Although the task of assessing handling qualities has not been formally addressed, some clear and useful impressions have been obtained which are believed to be pertinent to the full-scale aircraft. The model had unusually docile handling qualities throughout the portion of the flight envelope explored. On most flights, unplanned angle-of-sideslip and angle-of-attack excursions occurred that could have resulted in loss of control in a less forgiving model. This model was expected to be docile, so no special precautions were taken to strictly bound aerodynamic excursions. It has become apparent that the pilot is appreciably less aware of these excursions in remote piloting than in on-board piloting, and explicit measures will have to be taken in the remote piloting of less forgiving vehicles. There was some satisfaction from the experience and from the technical achievement, but in this situation the pilot is remote from the verifying and comforting sensations of flight.

CONCLUDING REMARKS

Exploratory glide flight tests of a three-eighth-scale fighter airplane model were made to validate the aerodynamic similarity of the model to the design and to check out the flight testing technique. The tests showed that the flight envelope could be quickly and safely expanded, stability and control data could be obtained over a wide range of conditions in relatively little flight time, controllability and handling could be investigated using normal piloting techniques, and configurations and controls could be quickly mechanized and flight tested.

Flight Research Center
National Aeronautics and Space Administration
Edwards, Calif., March 8, 1974

APPENDIX

SUMMARY OF PILOT COMMENTS

Impressions

"Remote pilot" is a more descriptive name than I had expected. Rather than detached, the feeling is remote from the essential verifying, comforting sensations of flight. After every unexpected event, the time taken to settle down is much longer than when the pilot is on board. I think this is because the verifying, confirming sensations are sparse, and they take more time to accumulate to a comfortable level than in flight. The difference between simulation and flight is enormous in this respect. Only the most superficial evidence that the flight is proceeding properly is quite enough in simulation, but in flight much more concrete and diverse evidence is demanded. In remote piloting this evidence is harder to come by.

I believe this was the source of the considerably greater work load in flight than in simulation, and the speedup of subjective time during actual flight. After the flight, we ran the simulator at 1.4 times real time. It seemed that events came upon the pilot at much the same pace as they had during the flight.

From the pilot's viewpoint, this remotely piloted flight was not pleasant or satisfying in the way a difficult or demanding real flight is. The results were gratifying, and some satisfaction was gained from the success of the technical and organizational achievement – but it wasn't fun.

Evaluation of Handling Qualities

This flight presented the opportunity to evaluate a few very simple, basic handling qualities. The up-and-away tasks – pitch steering and angle-of-attack trimming, bank steering, heading control, and roll in and out of turns – were evaluated. Because of the priority given to gathering aerodynamic data, there was no special time taken to assess and record the pilot's opinion of the various tasks. Fairly clear impressions of the vehicle handling qualities were retained and recorded, however. These were felt to be valid and reasonably representative of ratings that would have been obtained in flight. They are no doubt more valid than ratings based on simulation because of the greater fidelity of the aerodynamic simulation, but less valid than flight to the extent that the model flight control system and the ground cockpit control feel system are unrepresentative of the actual aircraft hardware.

It is my general impression that the faster time scale of the model does not have a large effect on the pilot ratings. Impressions gained in simulation, based on flying at various time scales, are that the individual tasks are not basically more difficult at fast time, but the pace of events becomes crowded.

Keeping in mind the conditions of the flight – statically and dynamically stable model, high quality control system, relatively good flying qualities, and up-and-away instrument tasks – the assessment of handling qualities seems feasible. [The pilot ratings assigned ranged from 4.5 for the high-dynamic-pressure, controls-unpleasantly-sensitive part of the flight immediately after launch to about 2 1/2 to 3 for the rolling maneuvers requested later in the flight at an angle of attack of about 22°. Generally the model control task was judged to be satisfactory for most of the flight envelope.]

Ground Cockpit

The ground cockpit was intended to provide a totally controlled environment. This was felt to be necessary because of the very strong state of concentration that characteristically developed during early remotely piloted flights. The ground cockpit did in fact provide the necessary isolation from all but essential stimuli. An estimate of the ground pilot's world, during flight, is as follows:

Flight attitude indicator	90 percent
Fine-scale angle of attack	2 percent
Flight controller	4 percent
Control pulser panel	2 percent
Flight engineer	1/2 percent
Airspeed	1/2 percent
Stick feel	1/2 percent
Angle-of-sideslip indicator	1/2 percent (only during initial trimming)

The flight attitude indicator display was extremely well suited to its required function, that is, providing attitude and heading information to the pilot. The remainder of the instrument panel seemed quite satisfactory in layout and in instrument face detail. The instruments appeared to function well, with the exception of the vertical velocity indicator, which was useless because of the large proportion of the time during which it was recovering from hard-overs. The annunciator panel and switchery were easy and natural to use. The mode control panel was really not satisfactory, but was usable. The only proper design of that panel is that any button should illuminate when depressed. The control pulser arrangement was absolute nonsense. The television had slightly degraded resolution but was generally satisfactory as it was. The television was unnecessary and distracting during the research maneuvers, but it was an aid at all other times.

The flight engineer function was unobtrusive and quite helpful. As expected, he monitored the progress of the maneuvers against the flight plan, prompting when necessary. He did the mode switching, and selected the next control surface to be pulsed. He also passed to the control room a commentary on what the pilot was doing.

The communications organization (and hardware) worked perfectly – exactly as hoped. The ground pilot got just the information needed but none extra. Because there was good rapport with the flight controller, it was somehow natural

and easy to respond to his commands in the degree required, but without being rigid to the detriment of completing the research maneuvers. All this about communications is important.

REFERENCES

1. Neihouse, Anshal I.; Klinar, Walter J.; and Scher, Stanley H.: Status of Spin Research for Recent Airplane Design. NASA TR R-57, 1960.

2. Chambers, Joseph R.: Status of Model Testing Techniques. Stall/Post-Stall/Spin Symposium, 15-17 December 1971, paper J. (Available only through Air Force Flight Dynamics Lab. (FGC), Wright-Patterson AFB, Ohio 45433.)

3. Edwards, John W.: Flight-Test of a Remotely Piloted Research Vehicle Using a Remote Digital Computer for Control Augmentation. Transactions of the first nwc symposium on the application of control theory to modern weapons systems — 9-10 May 1973. NWC TP 5522, Naval Weapons Center (China Lake, Calif.), June 1973, pp. 281-308.

4. Iliff, Kenneth W.; and Taylor, Lawrence W., Jr.: Determination of Stability Derivatives From Flight Data Using a Newton-Raphson Minimization Technique. NASA TN D-6579, 1972.

TABLE 1.– THREE-EIGHTH-SCALE MODEL CHARACTERISTICS

Total model –	
Wetted area, m^2 (ft^2)	34.87 (375.30)
Overall length, m (ft)	7.15 (23.45)
Wing –	
Area, m^2 (ft^2)	7.94 (85.50)
Span, m (ft)	4.89 (16.05)
Aspect ratio	3.0
Chord, m (ft):	
Root	2.60 (8.54)
Tip	0.65 (2.14)
Mean aerodynamic chord	1.82 (5.98)
Leading-edge sweep, deg	45
Taper ratio	0.25
Dihedral, deg	-1.0
Geometric twist, deg	0
Incidence, deg	0
Ailerons:	
Chord, m (ft) –	
Inboard edge	0.34 (1.11)
Outboard edge	0.22 (0.72)
Span, m (ft)	1.24 (4.06)
Percent of wing span	25.25
Deflection, deg	±20
Horizontal tail –	
Planform (exposed), m^2 (ft^2)	1.57 (16.88)
Aspect ratio	2.05
Taper ratio	0.34
Sweepback, deg:	
Leading edge	50.0
Quarter chord	43.55
Trailing edge	12.83
Chord, m (ft):	
Root	1.31 (4.29)
Tip	0.44 (1.46)
Mean aerodynamic chord	0.94 (3.10)
Dihedral, deg	0
Tail length, m (ft)	2.30 (7.53)
Deflection, deg:	
Total	15, -29
Symmetrical	15, -26
Differential	±11
Vertical tails –	
Area (both sides), m^2 (ft^2)	1.64 (17.61)
Span, m (ft)	1.18 (3.87)
Aspect ratio	1.70
Taper ratio	0.27

TABLE 1.– Concluded.

Sweepback, deg:	
Leading edge	36.57
Quarter chord	29.74
Trailing edge	3.45
Chord, m (ft):	
Root	1.09 (3.59)
Tip	0.29 (0.96)
Mean aerodynamic chord	0.77 (2.53)
Tail length, m (ft)	2.02 (6.63)
Rudders –	
Area (total), m^2 (ft^2)	0.26 (2.81)
Sweepback hinge line, deg	14.19
Span, m (ft)	0.54 (1.77)
Mean aerodynamic chord, m (ft)	0.24 (0.79)
Maximum deflection, deg	±30
Weight, N (lb)	10,964 (2465)
Moments of inertia –	
I_X, kg-m^2 (slug-ft^2)	373 (275)
I_Y, kg-m^2 (slug-ft^2)	2579 (1902)
I_Z, kg-m^2 (slug-ft^2)	3021 (2228)
I_{XZ}, kg-m^2 (slug-ft^2)	15.7 (11.6)
Center of gravity, percent mean aerodynamic chord	26

TABLE 2.– MODEL TELEMETRY PARAMETER LIST

(a) Model response parameters

Parameter	Range	Resolution	Prefilter frequency, Hz
Azimuth angle, deg –			
Sine	0 to 360	0.70	40
Cosine	0 to 360	0.70	40
Roll angle, deg –			
Sine	0 to 360	0.70	40
Cosine	0 to 360	0.70	40
Pitch angle, deg –			
Sine	0 to 360	0.70	40
Cosine	0 to 360	0.70	40
Azimuth angle, deg –			
Sine	315 to 45	0.18	40
Cosine	315 to 45	0.18	40
Roll angle, deg –			
Sine	315 to 45	0.18	40
Cosine	315 to 45	0.18	40
Pitch angle, deg –			
Sine	335 to 25	0.10	40
Cosine	335 to 25	0.10	40
Roll rate, deg/sec	±200	0.78	40
Roll rate, deg/sec	±50	0.20	40
Pitch rate, deg/sec	±100	0.39	40
Pitch rate, deg/sec	±25	0.10	40
Yaw rate, deg/sec	±100	0.39	40
Yaw rate, deg/sec	±25	0.10	40
Normal acceleration, g	-3 to 6	0.018	40
Normal acceleration, g	±2	0.01	40
Longitudinal acceleration, g	±1	0.004	40
Lateral acceleration, g	±1	0.004	40
Angle of attack, deg	89 to -9	0.19	40
Angle of attack, deg	±20 at 15	0.05	40
Angle of attack, deg	±12.5 at 37.5	0.05	40
Angle of sideslip, deg	±60	0.23	40
Angle of sideslip, deg	±20	0.08	40
Airspeed, knots –			
Coarse	35 to 350	0.62	40
Fine	31.5 per turn	0.06	40
Altitude, m (ft) –			
Coarse	0 to 16,886 (55,400)	33 (108)	40
Fine	1829 (6000) per turn	3.6 (11.7)	40
Left horizontal stabilizer, deg	15 to -29	0.10	40
Right horizontal stabilizer, deg	15 to -29	0.10	40
Left rudder, deg	±30	0.12	40
Right rudder, deg	±30	0.12	40
Left aileron, deg	±20	0.08	40
Right aileron, deg	±20	0.08	40

TABLE 2.– Concluded.

(b) Operational parameters

Parameter	Range
Battery current, amperes –	
Number 1	0 to 100
Number 2	0 to 200
Battery voltage, volts –	
Number 1	0 to 41
Number 2	0 to 41
Power supply monitor, volts dc	6
Power supply monitor, volts dc	-6
Power supply monitor, volts dc	15
Power supply monitor, volts dc	-15
Power supply monitor, volts ac	0 to 26
Hydraulic pump pressure	- - - -
Instrument compartment temperature	- - - -
Battery compartment temperature	- - - -

(c) Discrete signals

Airplane mode
Launch mode
Hydraulic pump pressure low
Radio frequency carrier loss – number 1; number 2
MARS not armed – number 1; number 2
Parachute deploy – number 1; number 2
Barometric switch position, 4572 meters (15,000 feet) – number 1; number 2
Barometric switch position, 1524 meters (5000 feet) – number 1; number 2

TABLE 3.– TELEMETRY DOWNLINK SPECIFICATIONS

160,000 bits per second
9 bits per word
80 words per PCM frame
200 PCM frames per second
No parity check
L-band transmission
3.66-meter (12-foot) parabolic receiving antenna slaved to radar tracking antenna

TABLE 4.– COMPUTER EQUIPMENT

Peripheral equipment:
- Card reader
- Disc unit
- Line printer
- Magnetic-tape unit
- Teletype
- Paper-tape reader/punch
- Peripheral floating point hardware unit

Software:
- Assembler
- FORTRAN IV compiler
- Mathematical subroutine support library

Main-frame options:
- Automatic bootstrap loader
- Real-time clock
- Power/fail restart
- Priority interrupt module
- Direct-memory access unit

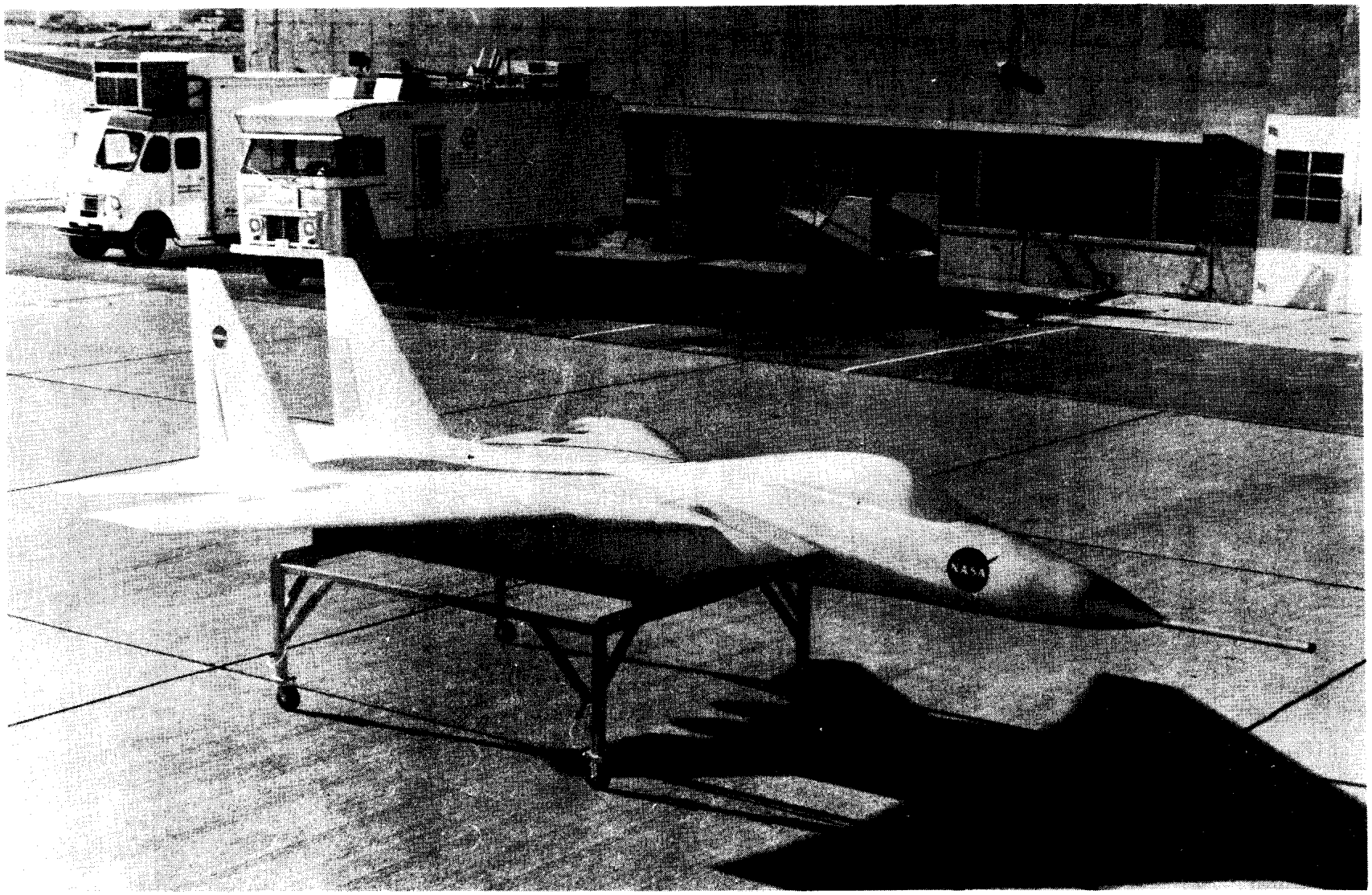

Figure 1. Three-eighth-scale model. E-25487

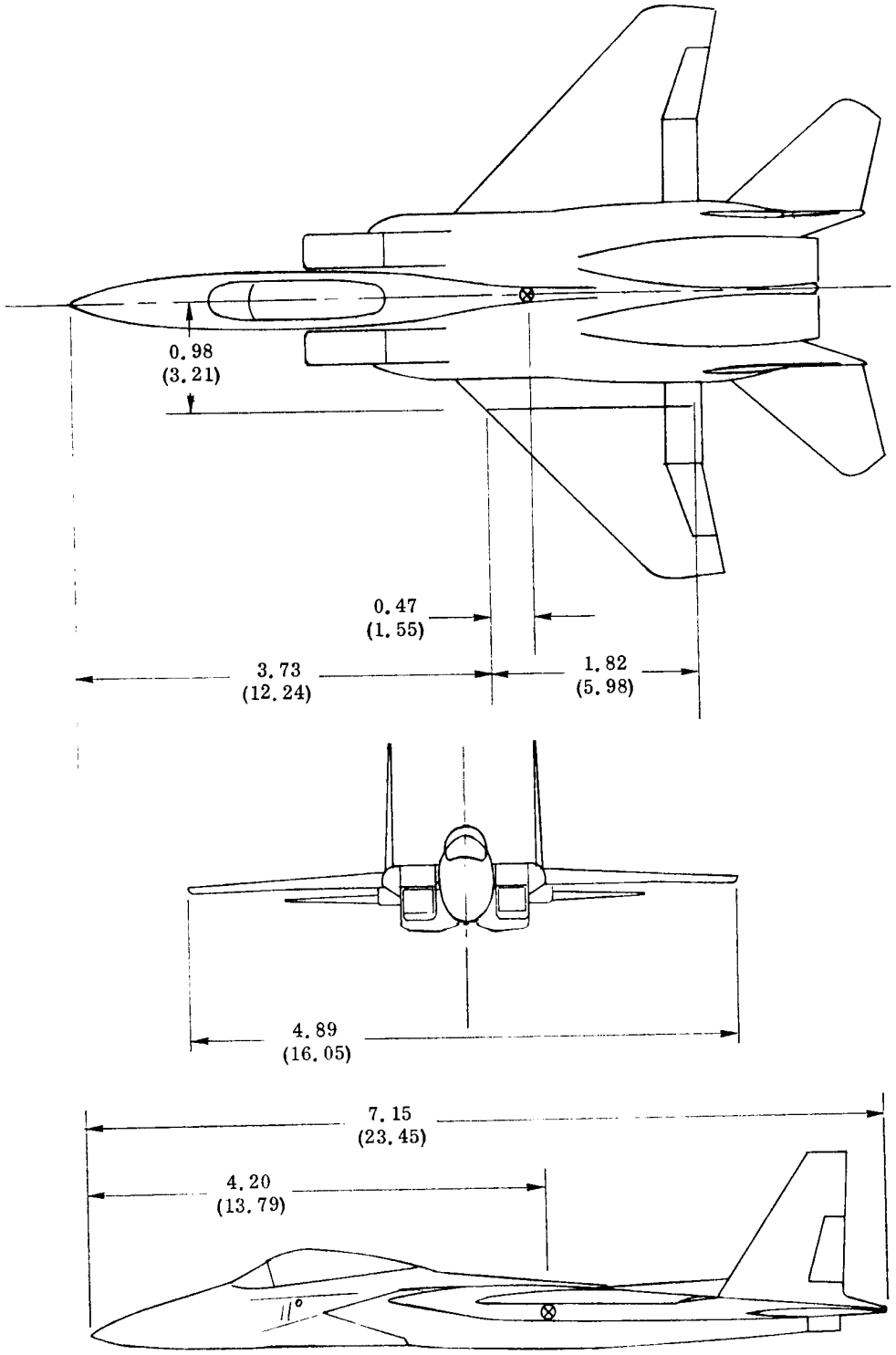

Figure 2. Three-view drawing of model. Dimensions in meters (feet).

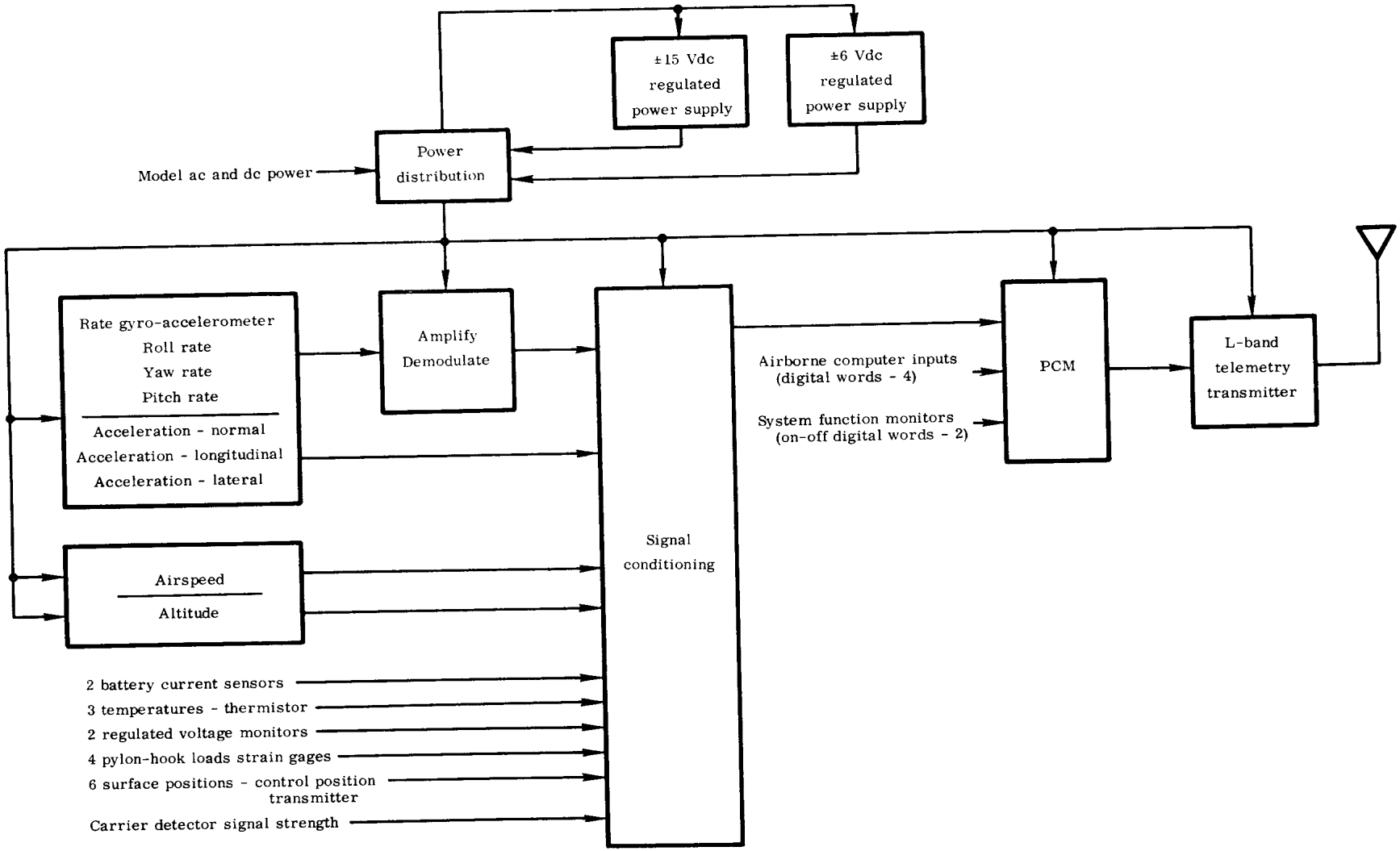

Figure 3. Block diagram of the model instrumentation system.

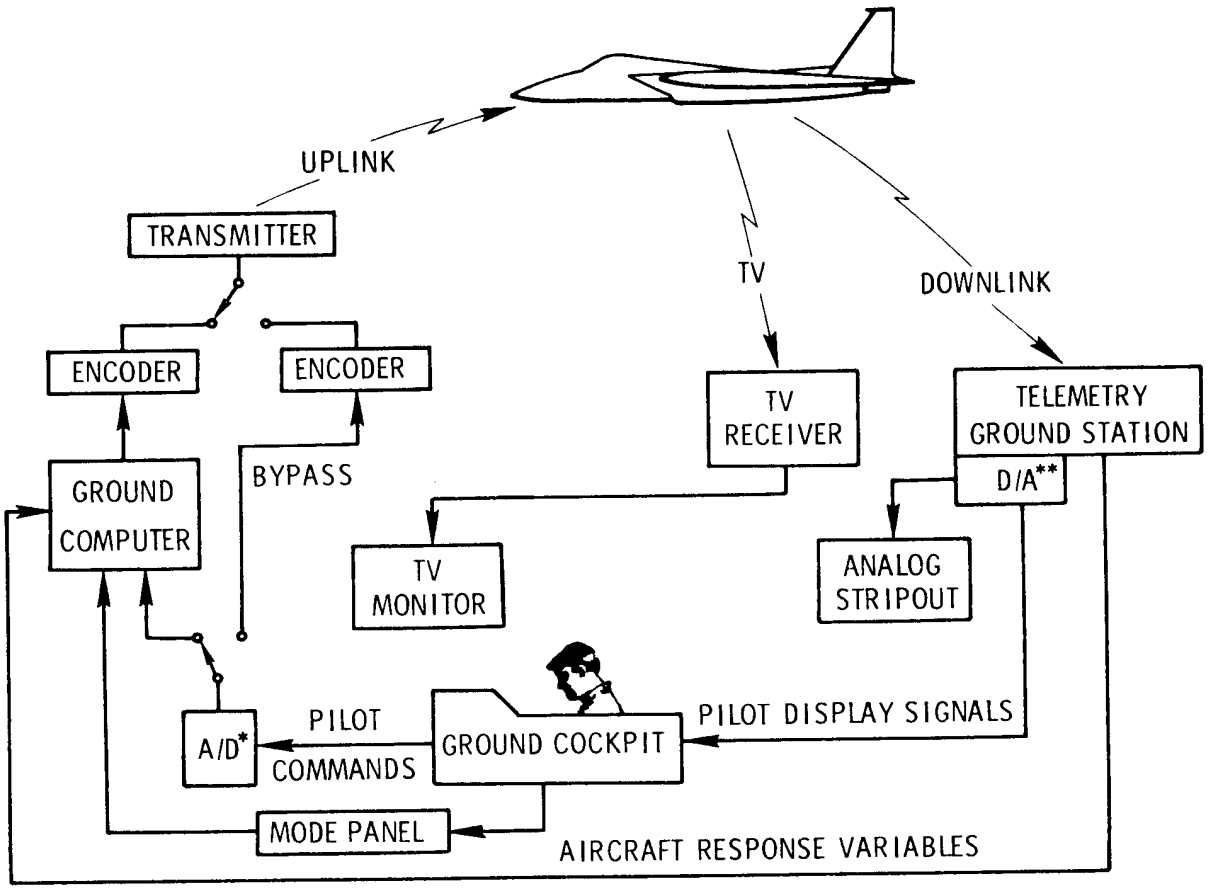

*Analog-to-digital

**Digital-to-analog

Figure 4. Remotely piloted model control loops.

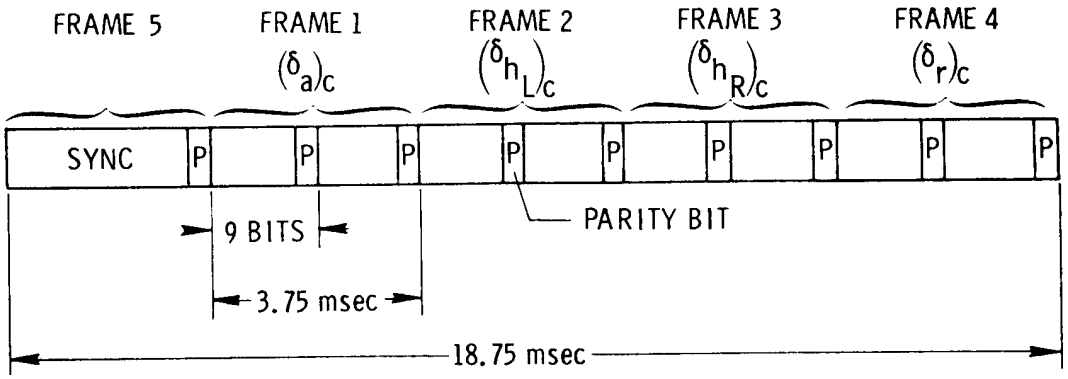

Figure 5. Telemetry uplink time schedule.

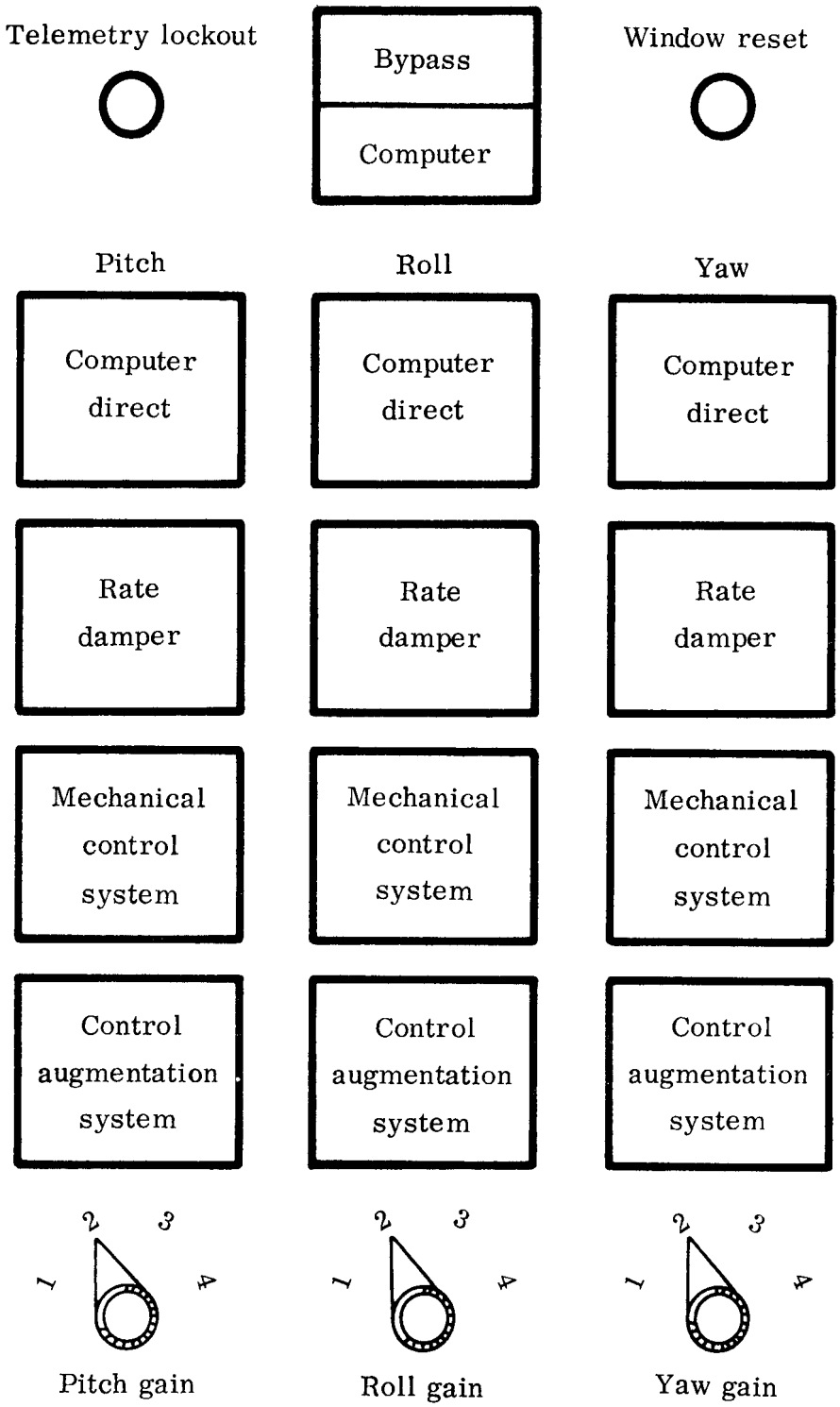

Figure 6. Model control mode panel.

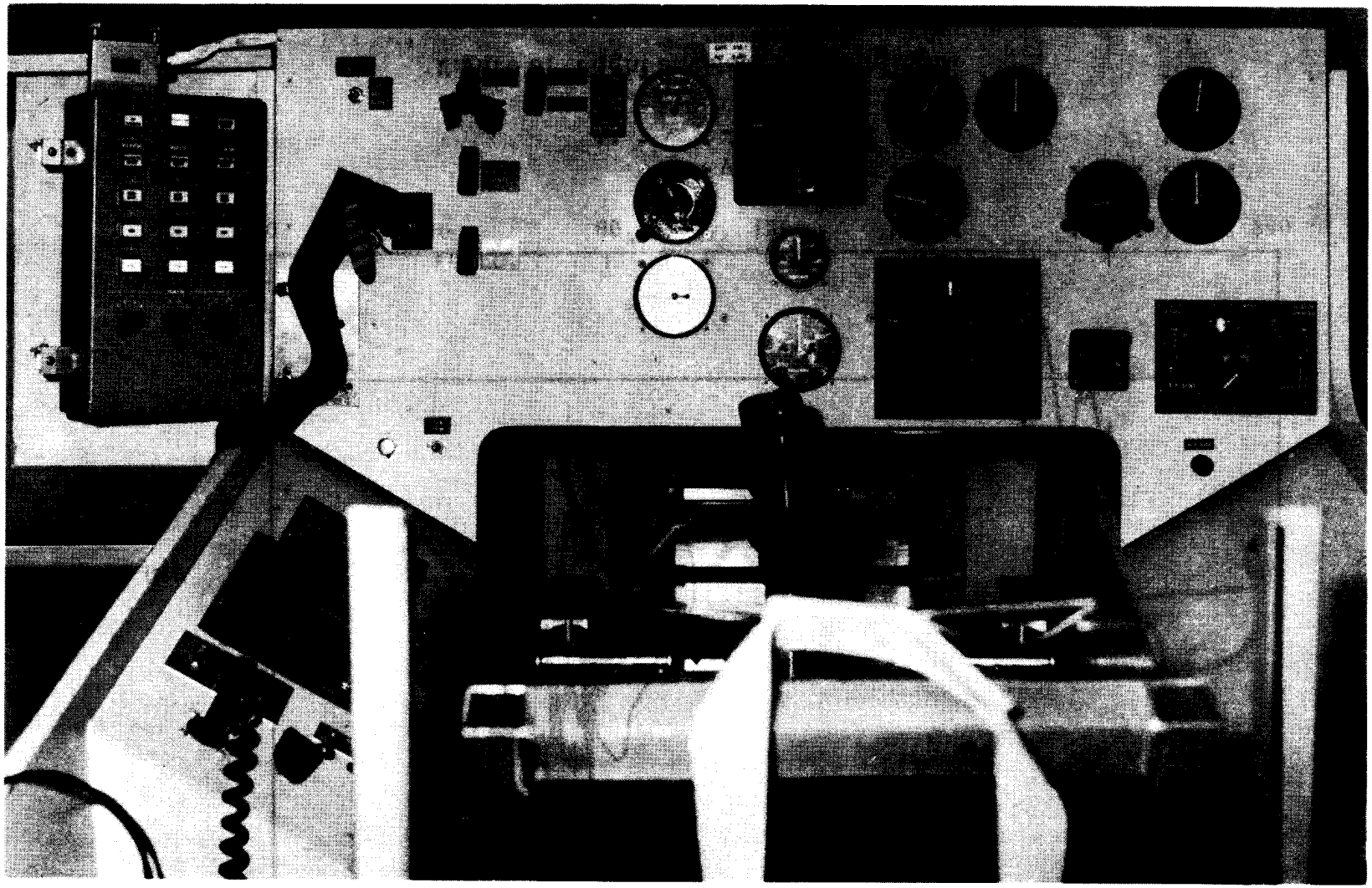

Figure 7. Pilot's control station. E-26991

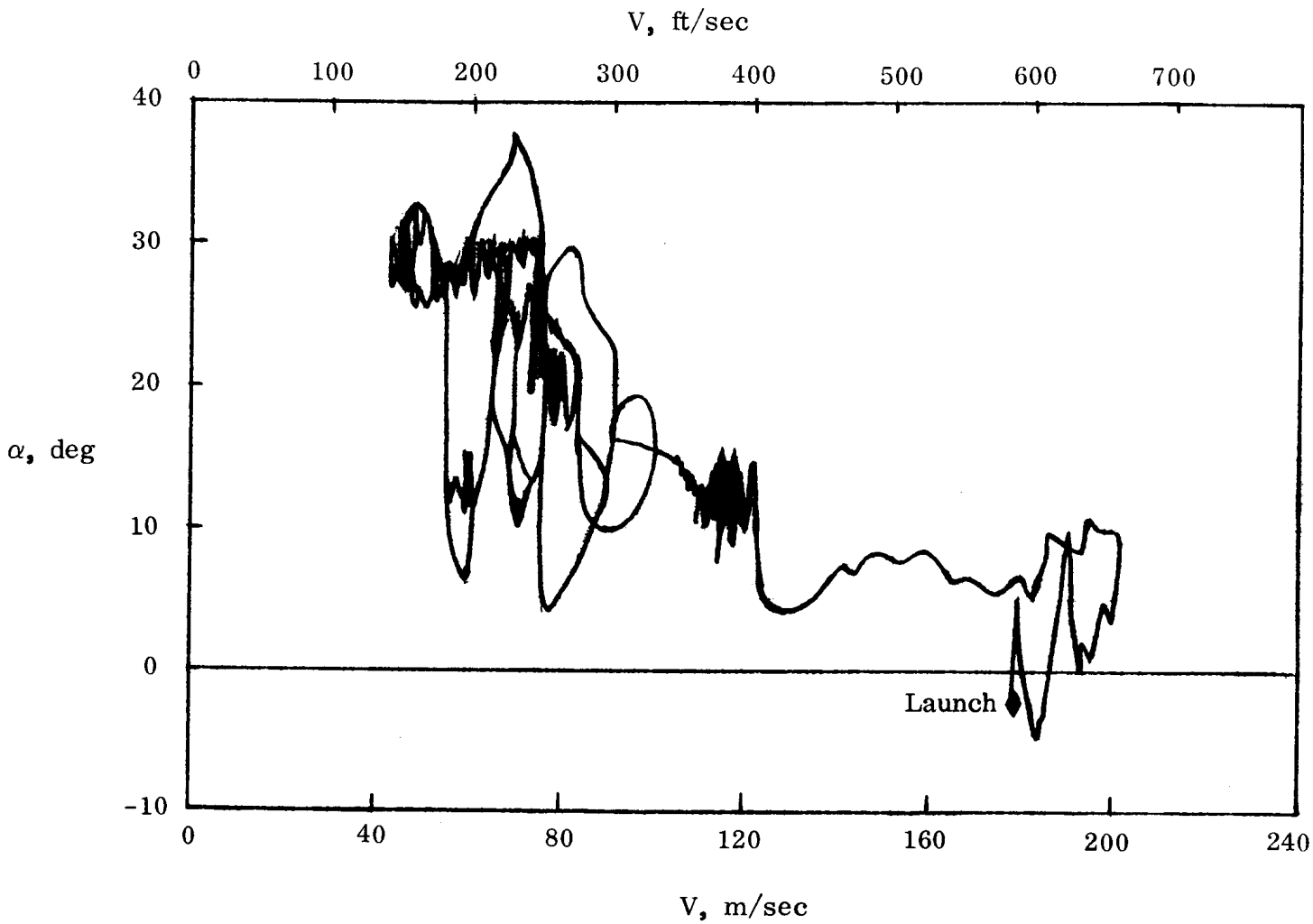

Figure 8. Flight envelope of third flight.

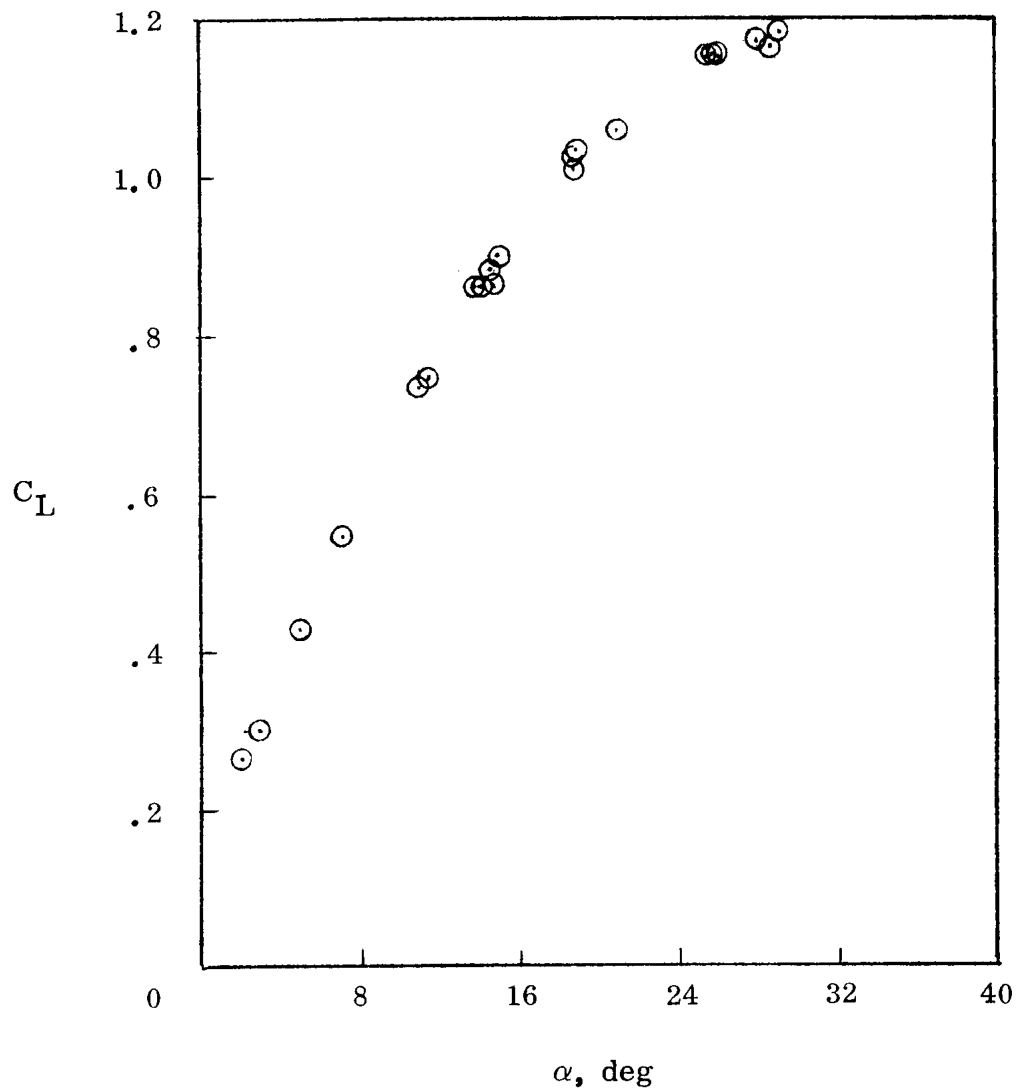

Figure 9. Lift variation with angle of attack obtained during one flight. $q \leq 0.2$ deg/sec.

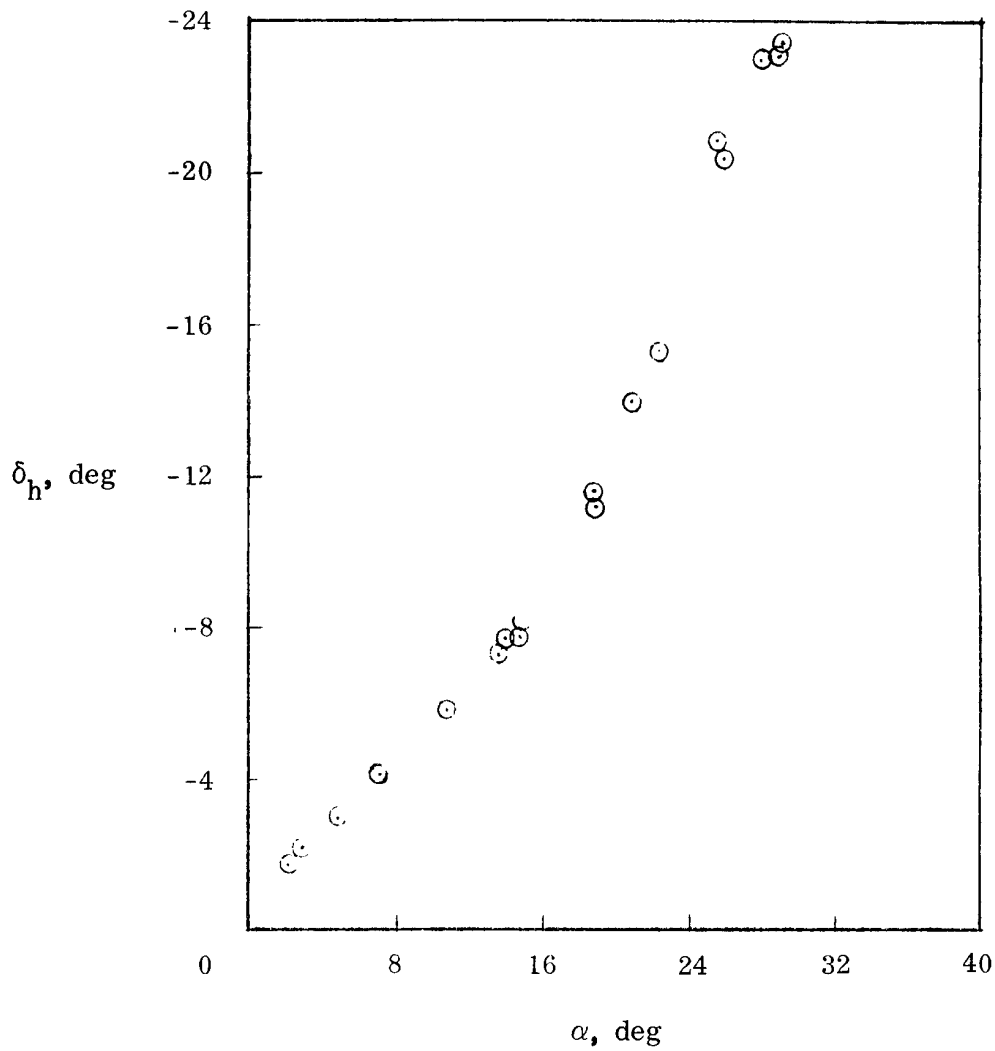

Figure 10. Longitudinal control required to trim model angle of attack. Center of gravity = 26 percent; $q \leq 0.2$ deg/sec.

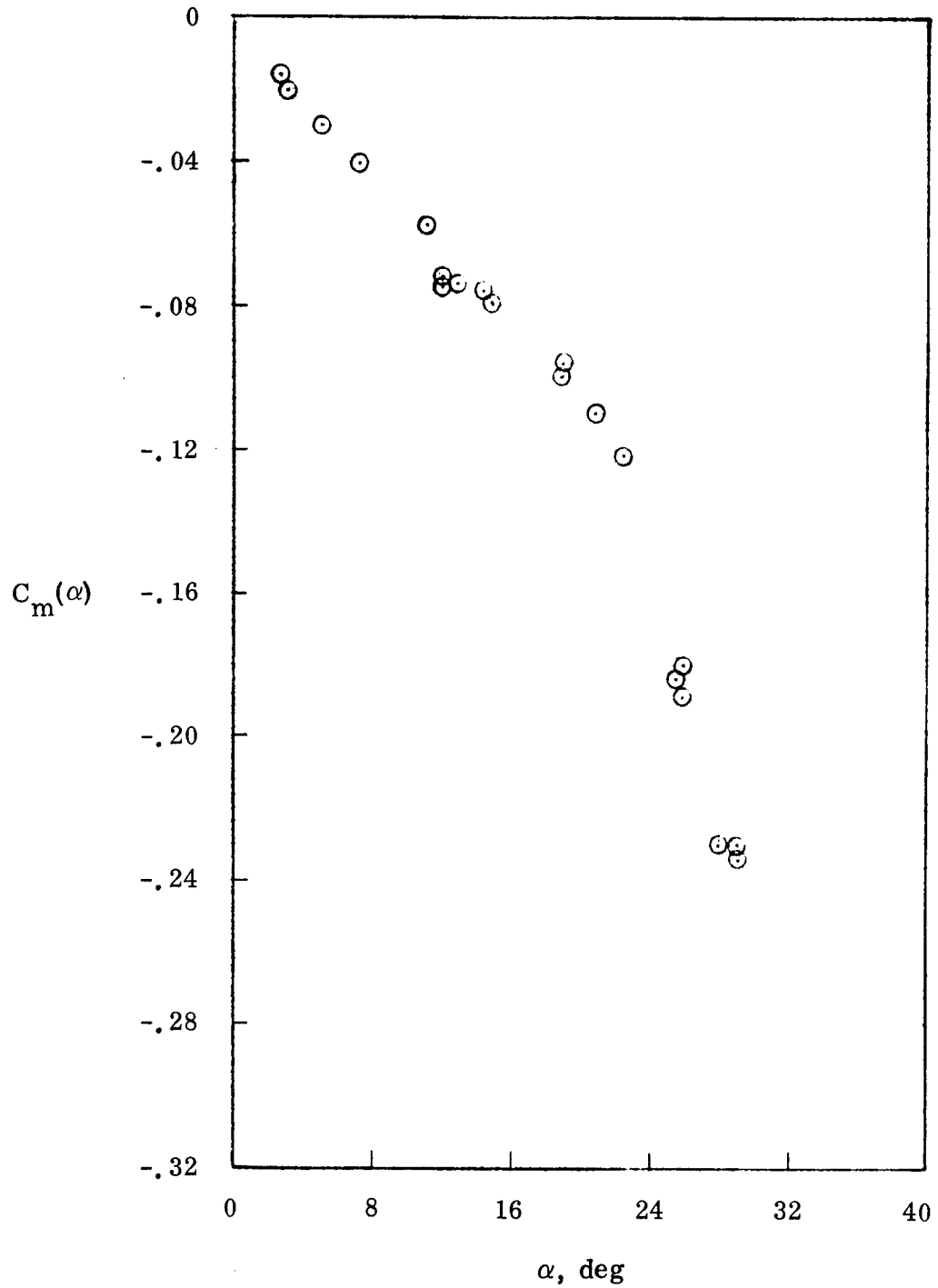

Figure 11. Pitching moment coefficient for angles of attack up to 28°. Center of gravity = 26 percent; $q \leq 0.2$ deg/sec.

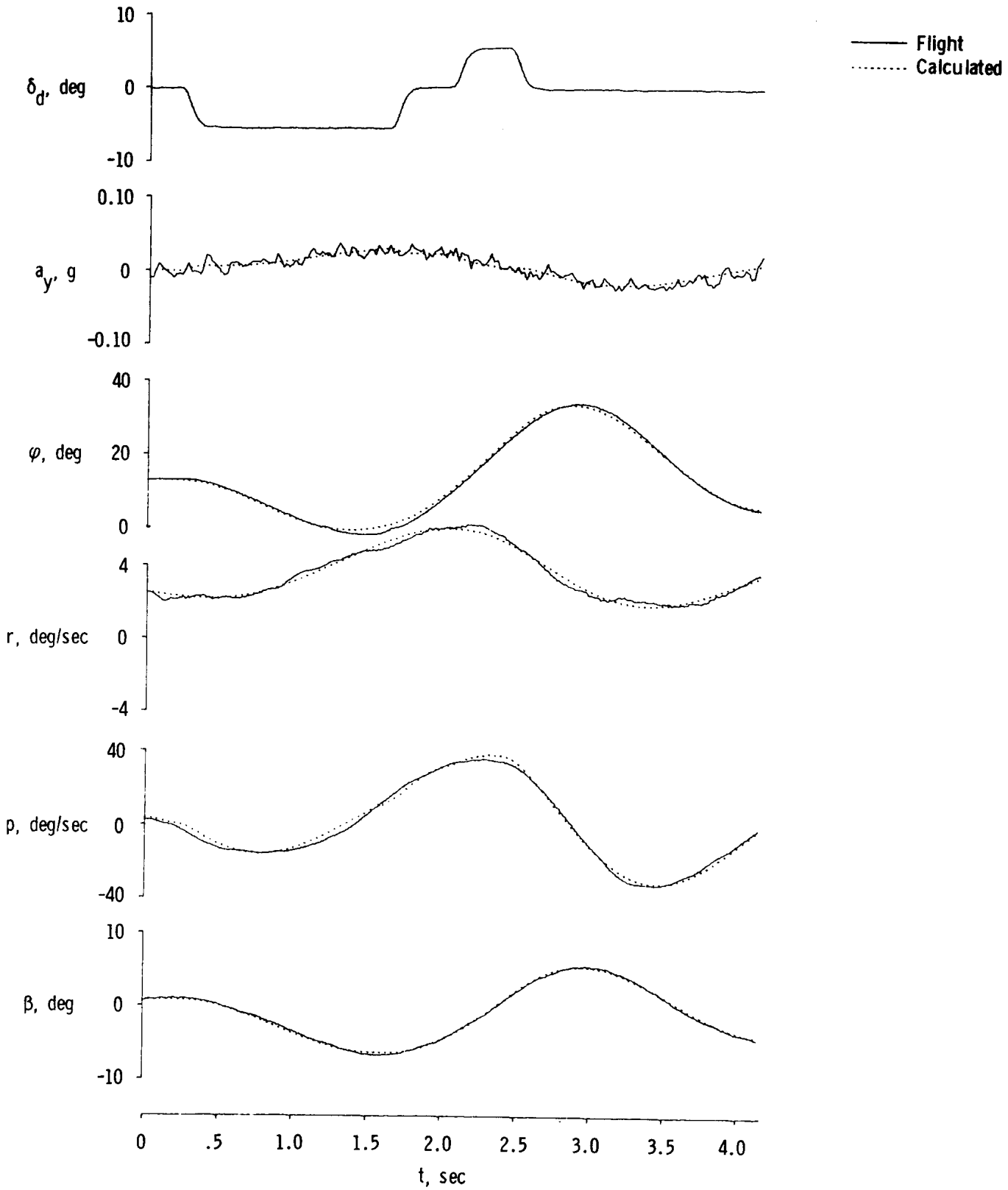

(a) Lateral maneuver.

Figure 12. Comparison of typical flight data and computed time histories based on the estimated derivatives.

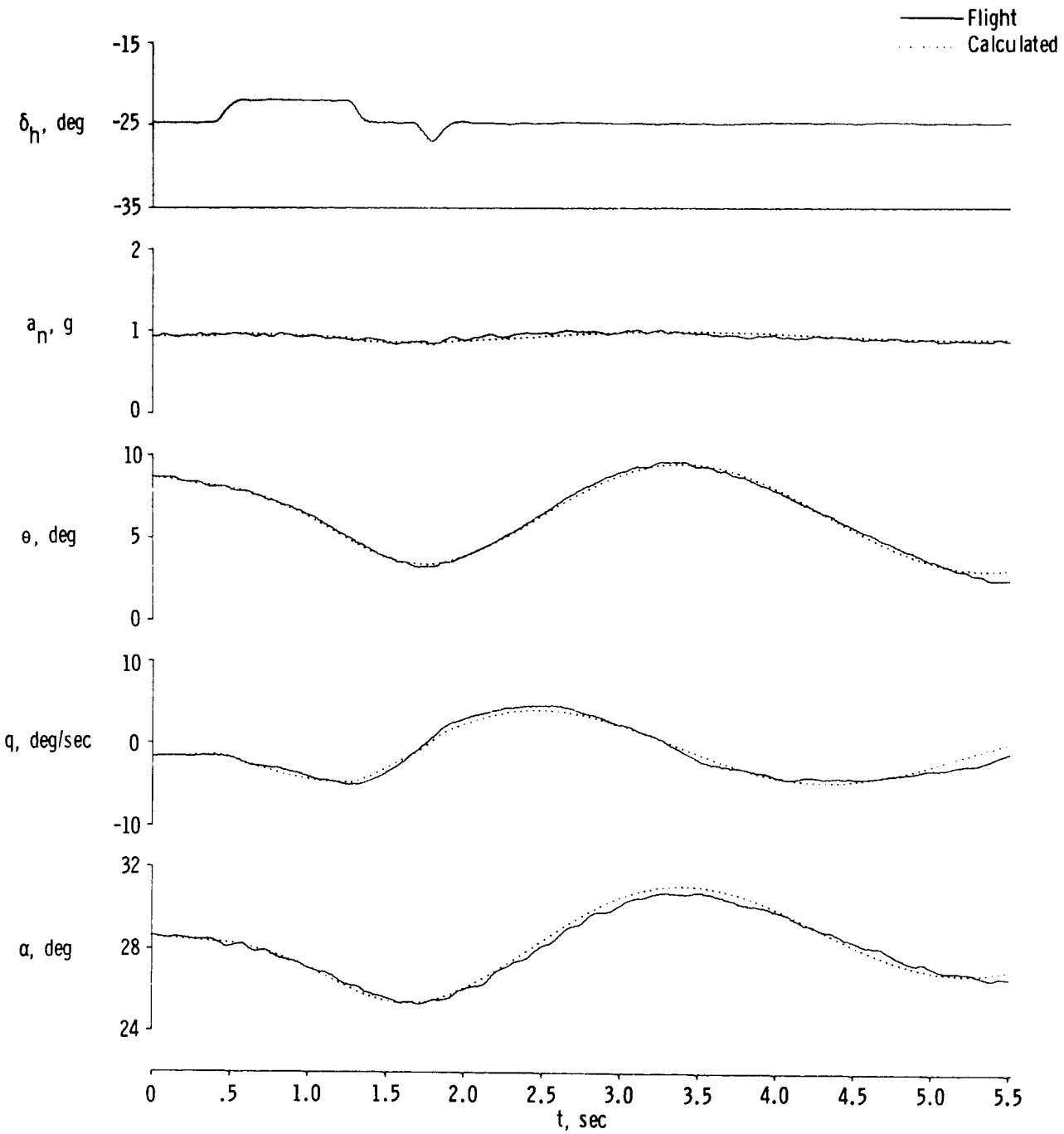

(b) Longitudinal maneuver.

Figure 12. Concluded.

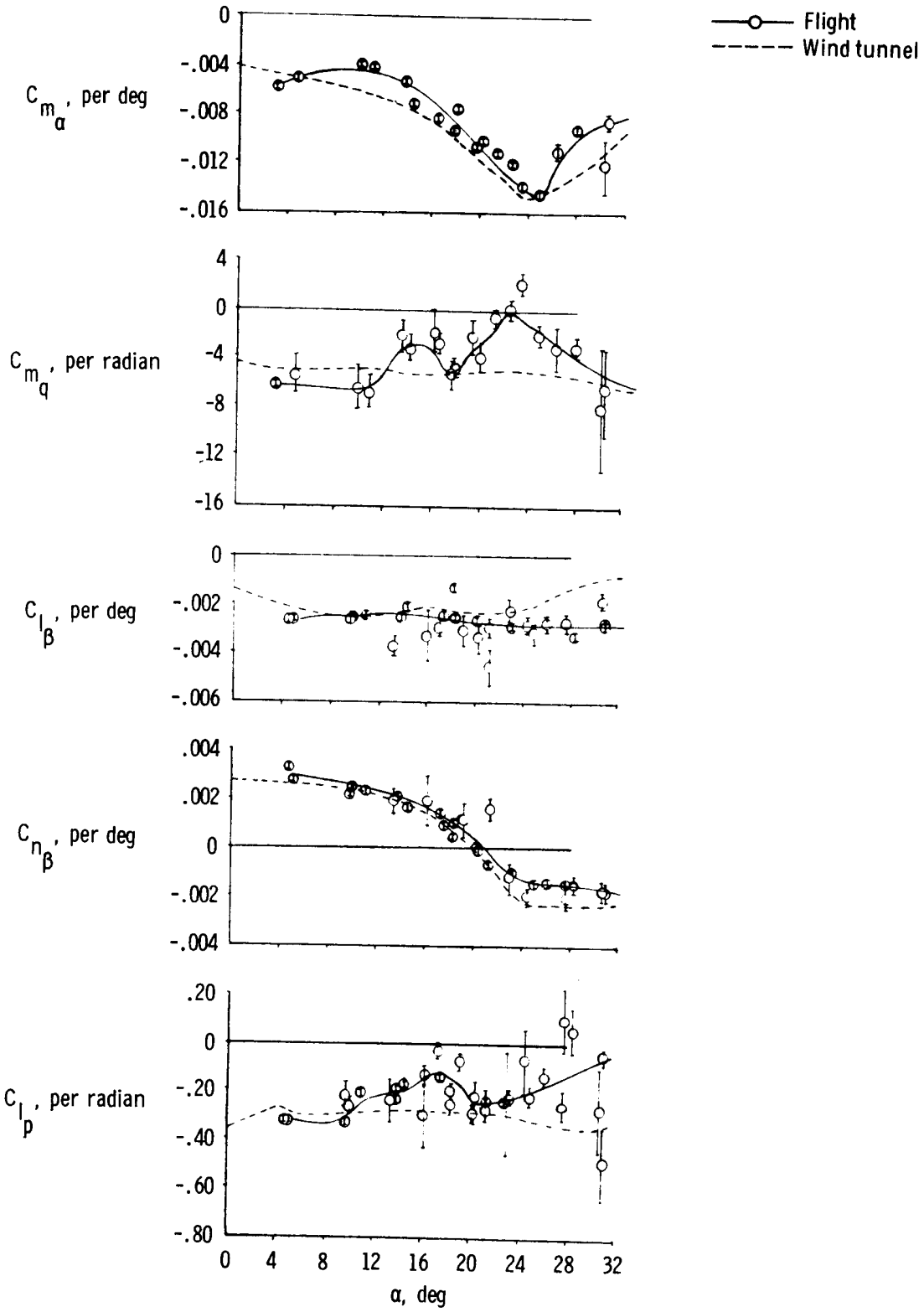

Figure 13. Comparison of flight and wind-tunnel estimates for five stability derivatives. Vertical lines indicate confidence levels.

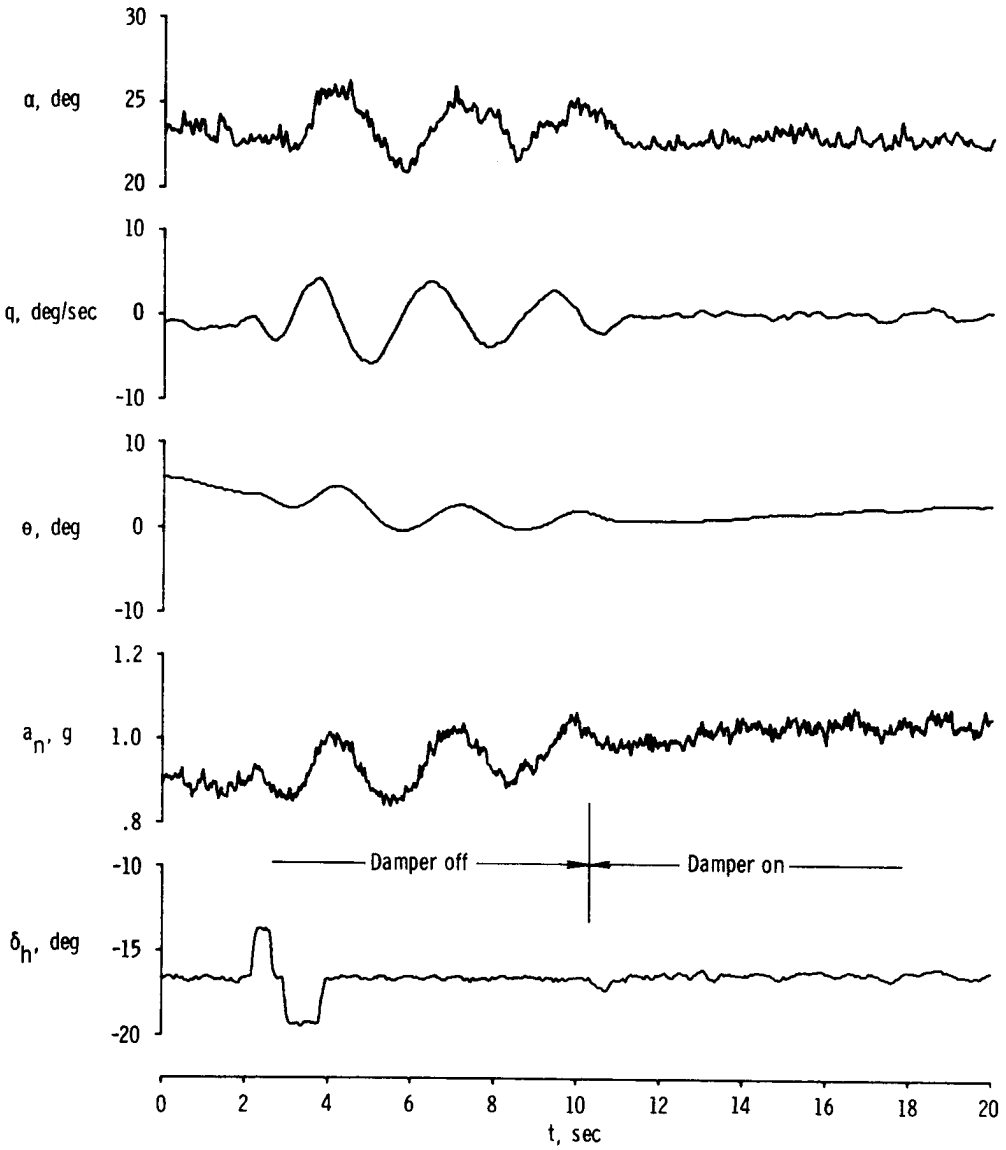

(a) Pitch rate damper. Damper gain, 0.4 deg/deg/sec.

Figure 14. Operation of rate dampers during flight 4.

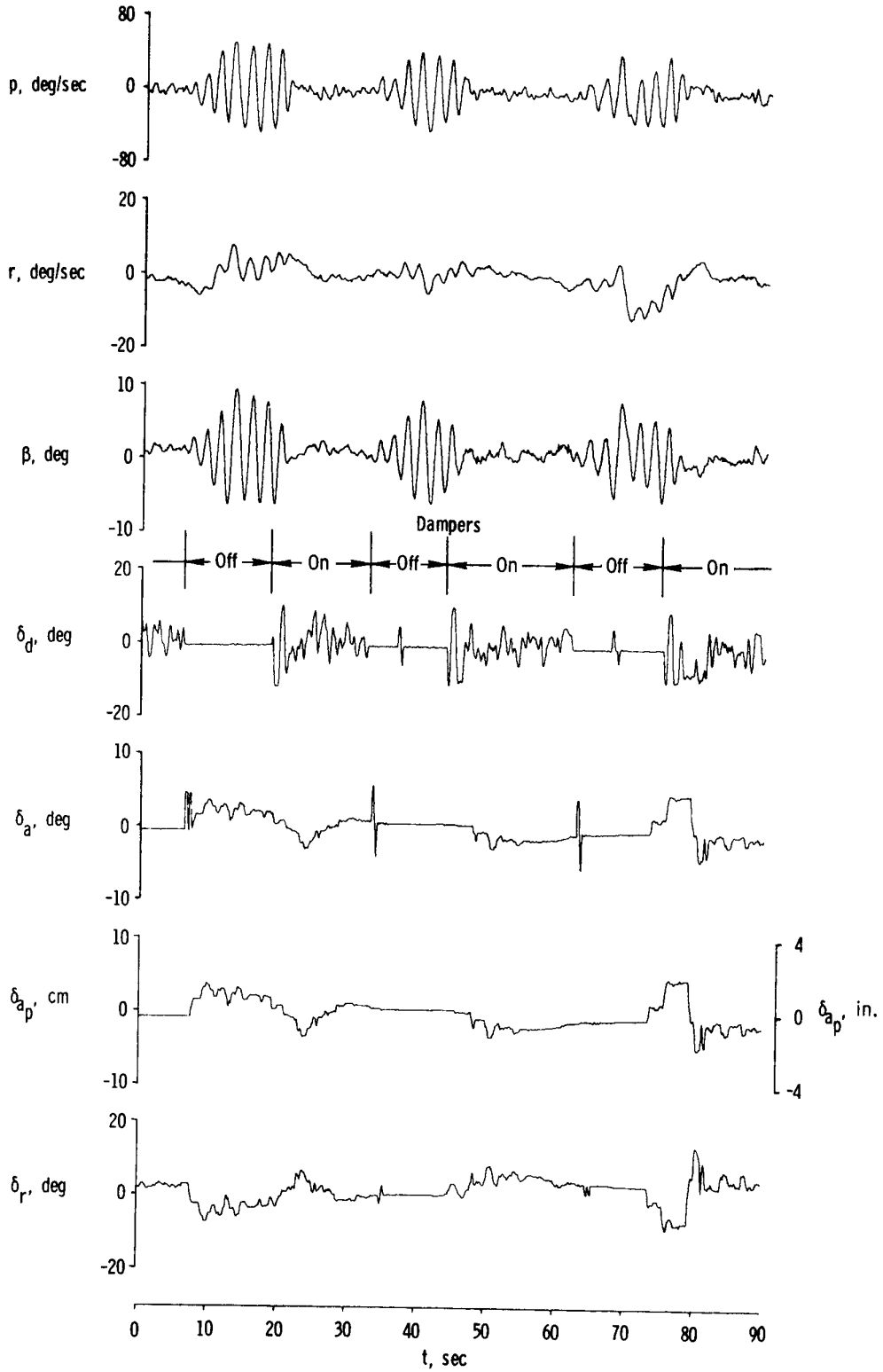

(b) Roll and yaw rate dampers (α = 28° to 31°). Roll damper gain, 0.8 deg/deg/sec; yaw damper gain, 1.0 deg/deg/sec.

Figure 14. Concluded.

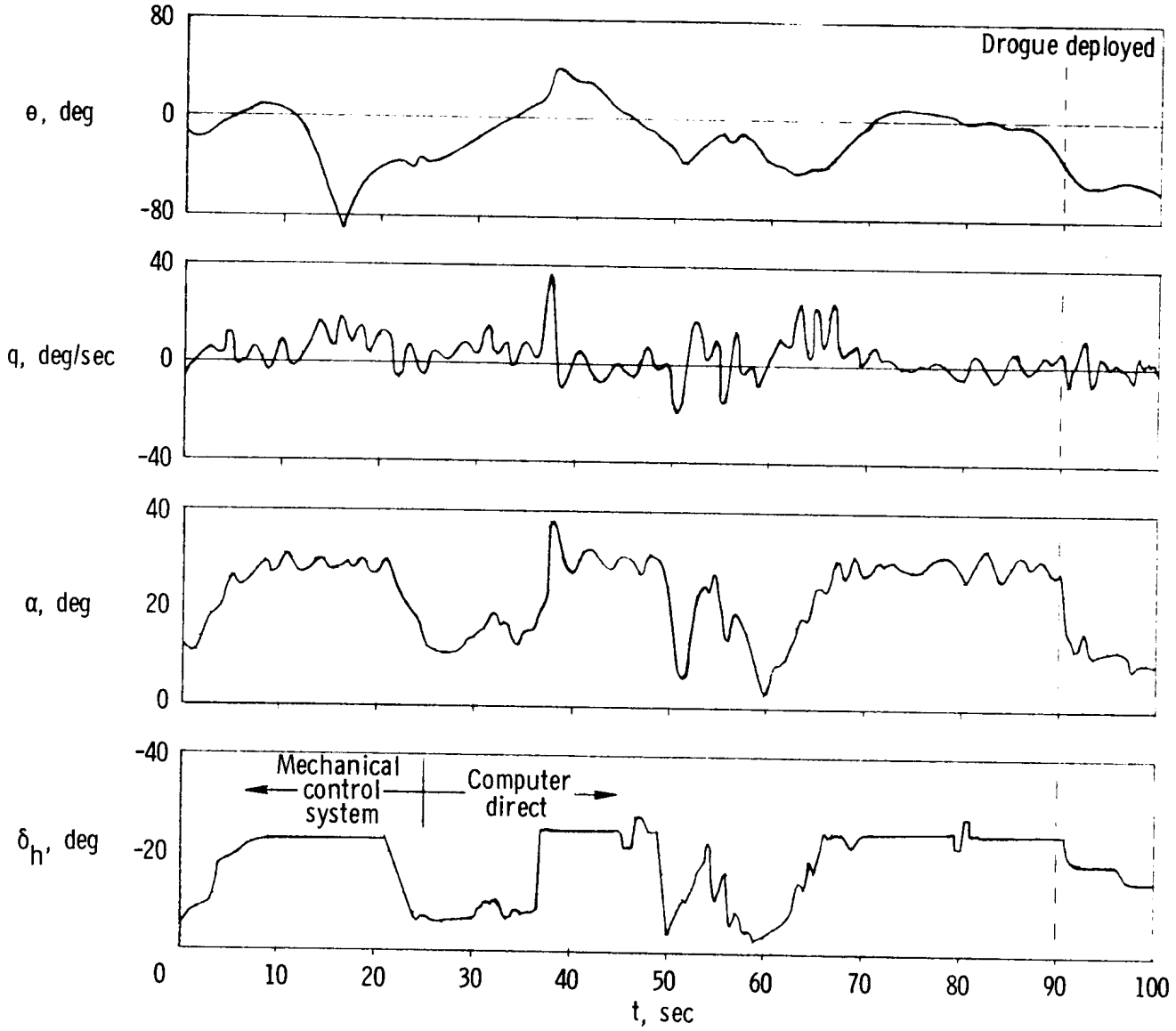

(a) Pitch quantities.

Figure 15. Investigation of controllability at high angle of attack.

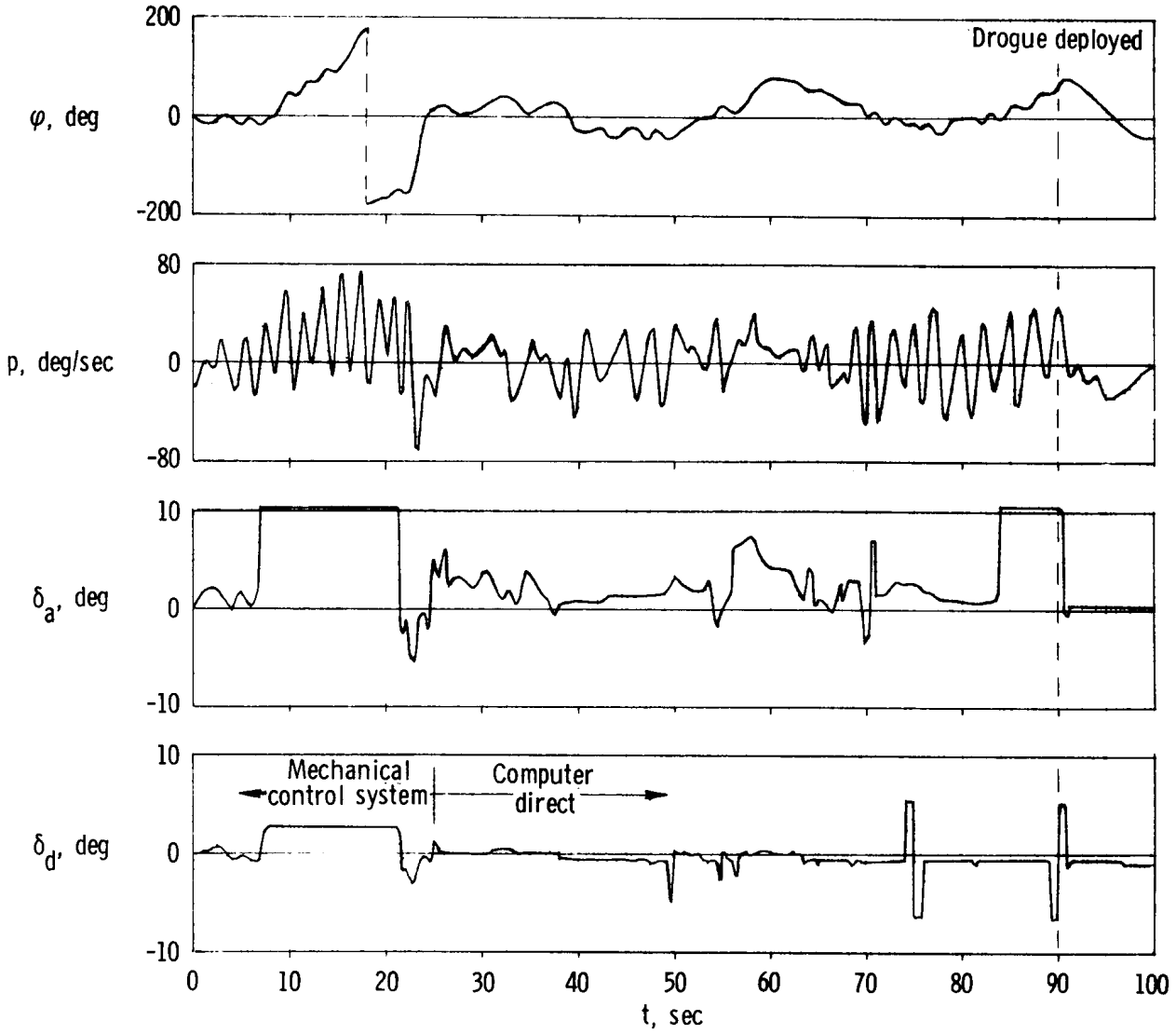

(b) Roll quantities.

Figure 15. Continued.

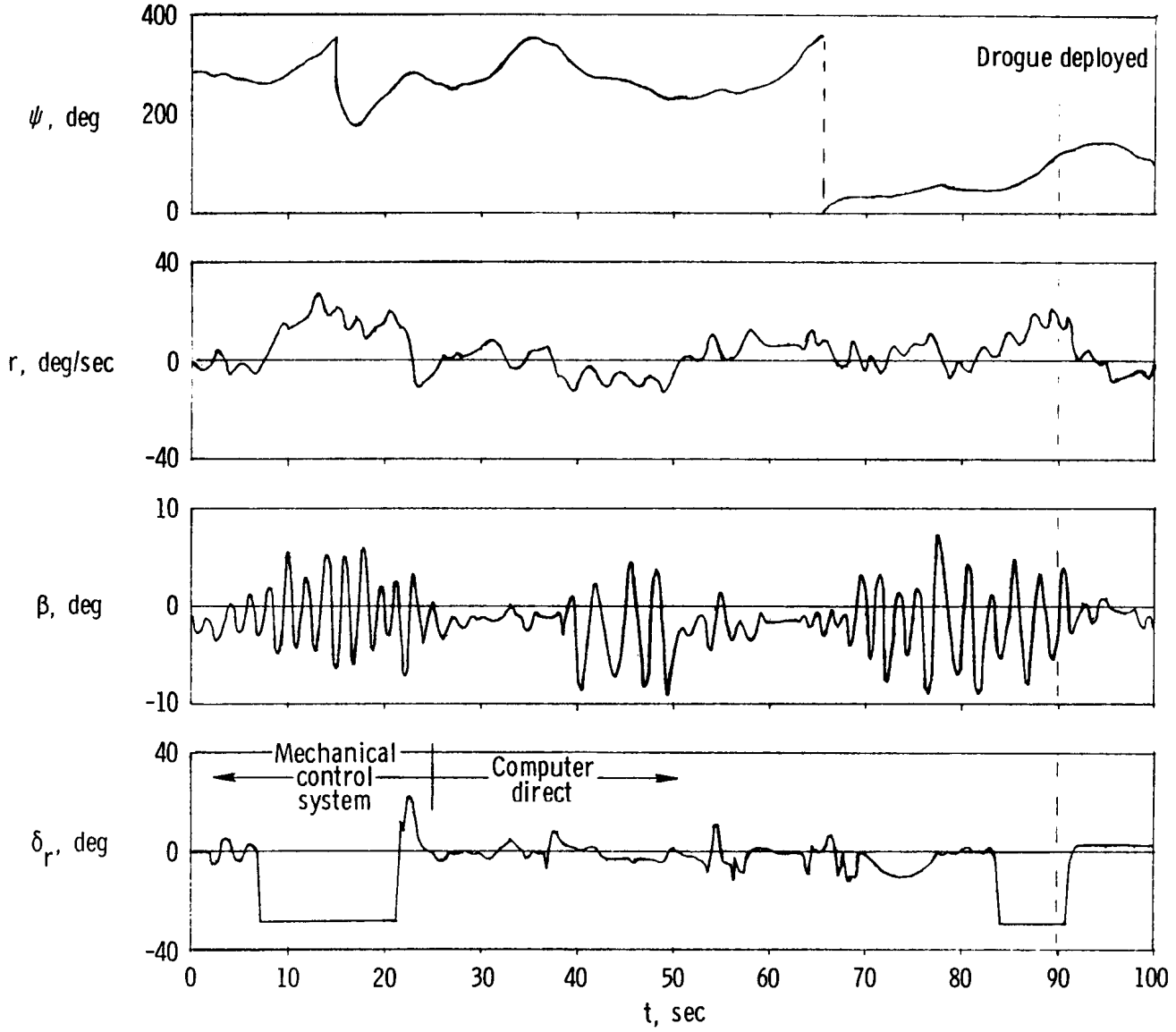

(c) Yaw quantities.

Figure 15. Concluded.